Physical and chemical characterization of urban winter-time aerosols by mobile measurements in Helsinki, Finland

Liisa Pirjola[a,b*], Jarkko V. Niemi[c,d], Sanna Saarikoski[e], Minna Aurela[e], Joonas Enroth[b], Samara Carbone[e,+], Heino Kuuluvainen[f], Anu Kousa[c], Topi Rönkkö[f], Risto Hillamo[e]

[a]Department of Technology, Metropolia University of Applied Sciences, P.O. Box 4021, FI-00180 Helsinki, Finland

[b]Department of Physics, University of Helsinki, P. O. Box 64, FI-00014 Helsinki, Finland

[c]Helsinki Region Environmental Services Authority HSY, P.O. Box 100, FI-00066 HSY, Helsinki, Finland

[d]Department of Environmental Sciences, University of Helsinki, P.O. Box 65, FI-00014 Helsinki, Finland

[e]Air Quality, Finnish Meteorological Institute, P.O. Box 503, FI-00101 Helsinki, Finland

[f]Department of Physics, Tampere University of Technology, P.O. Box 692, FI-33101 Tampere, Finland

+now at Institute of Agrarian Sciences, Federal University of Uberlandia, Uberlandia, Brazil

[*]Corresponding author: Email address liisa.pirjola@metropolia.fi; liisa.pirjola@helsinki.fi (L.Pirjola)

Submitted 30.11.2016 to Atmospheric Environment

Highlights

- four distinct sources and corresponding characteristics of aerosols were identified
- size distributions of particle number and lung deposited surface area were measured
- OOA and inorganics dominated chemical composition during long-range transport episode
- BC, HOA and BBOA dominated local traffic and wood burning emissions
- high amounts of K/S/C-rich and soot particles were detected in small house areas

Abstract

A two-week measurement campaign by a mobile laboratory van was performed in urban environments in the Helsinki metropolitan area, Finland, in winter 2012, to obtain a comprehensive view on aerosol properties and sources. The abundances and physico-chemical properties of particles varied strongly in time and space, depending on the main sources of aerosols. Four major types of winter aerosol were recognized: 1) clean background aerosol with low particle number (Ntot) and lung deposited surface area (LDSA) concentrations due to marine air flows from the Atlantic Ocean; 2) long-range transported (LRT) pollution aerosol due to air flows from eastern Europe where the particles were characterized by the high contribution of oxygenated organic aerosol (OOA) and inorganic species, particularly sulphate, but low BC contribution, and their size distribution possessed an additional accumulation mode; 3) fresh smoke plumes from residential wood combustion in suburban small houses, these particles were characterized by high biomass burning organic aerosol (BBOA) and black carbon (BC) concentrations; and 4) fresh emissions from traffic while driving on busy streets in the city centre and on the highways during morning rush hours. This aerosol was characterized by high concentration of Ntot, LDSA, small particles in the nucleation mode, as well as high hydrocarbon-like organic aerosol (HOA) and BC concentrations. In general, secondary components (OOA, NO_3, NH_4, and SO_4) dominated the PM_1 chemical composition during the LRT episode accounting for 70-80% of the PM_1 mass, whereas fresh primary emissions (BC, HOA and BBOA) dominated the rest of the campaign. The major individual particle types observed with electron microscopy analysis (TEM/EDX) were mainly related to residential wood combustion (K/S/C-rich, soot, other C-rich particles), traffic (soot, Si/Al-rich, Fe-rich), heavy fuel oil combustion in heat plants or ships (S with V-Ni-Fe), LRT pollutants (S/C-rich secondary particles) and sea salt (Na/Cl-rich). Tar balls from wood combustion were also observed, especially (~5%) during the LRT pollution episode.

Keywords: mobile laboratory, traffic, wood burning, size distribution, black carbon, AMS

1. Introduction

In urban and suburban areas particle emissions from traffic and wood combustion are known to significantly contribute to regional air quality (e.g. EEA, 2015) and the Earth's radiation budget (IPCC, 2013). Aerosol particles directly affect climate by scattering or absorbing incoming solar radiation and indirectly by influencing cloud processes. Although the radiative forcing of the total aerosol effect in the atmosphere is negative, the radiative forcing due to black carbon (BC) absorption of solar radiation is positive (IPCC, 2013). Additionally, black carbon on snow and ice in the Arctic increase the melting of snow and ice cover and consequently increase climate warming (Quinn et al., 2008; Hirdman et al. 2010; AMAP, 2011; Bond et al., 2013). BC particles from diesel emissions and wood combustion contain carcinogenic and mutagenic agents, and they have been linked to increased complications in cardiovascular and respiratory systems (Pope et al., 2006; Su et al., 2008; Alföldy et al., 2009; Naeher et al., 2007; Poulain et al., 2011). In toxicological studies the surface area of particles has been shown to correlate with inverse health effects (Brown et al., 2001; Oberdörster et al., 2005).

During the past 10 years the quantitative determination of wood burning and traffic emission contributions to particulate matter (PM) has been intensively studied in Central Europe and Scandinavia, particularly because of the development of novel instruments such as the multi-wavelenth aethalometer for black carbon mass and the aerosol mass spectrometer (AMS) for chemical particle composition measurements. Residential wood combustion (RWC) for domestic heating is increasing in Europe due to the reduction in the use of fossil fuels and climate change mitigation policies (Denier van der Gon et al., 2015). RWC is the largest source of organic aerosol (OA) in the Alpine region in Europe (Denier van der Gon et al., 2015), accounting on average for 17-49% of the total organic aerosol (OA) in wintertime (Lanz et al., 2010). For example, based on AMS measurements in winter the biomass burning OA comprised 20% of the total OA mass in Seiffen, Germany (Poulain et al., 2011), 37-68% in Grenoble, France (Favez et al., 2010), ~88% in Roveredo, Switzerland (Alfarra et al., 2007; Sandradewi et al., 2008), and 49% of $PM_{2.5}$ in Mlada Boleslav in Czeck Republic (Hovorka et al., 2015). Mohr et al. (2011) discovered during their wintertime mobile measurements in the vicinity of Zürich, Switzerland, that on average the organic fraction accounted for one third of PM_1, and was dominated by oxygenated organic aerosol (OOA), followed by wood burning organic aerosol (WBOA) and hydrocarbon-like organic aerosol (HOA). They also observed that on major traffic roads BC could account for 35% of PM_1.

In a small village in Northern Sweden, RWC and traffic explained high evening concentrations of particulate matter, BC and particle number in winter (Kreck et al., 2008).

In Finland, RWC comprised ~55% of total BC emissions, traffic being the next largest BC source in 2010 (Savolahti et al., 2016). In the Helsinki metropolitan area, the contributions of different PM emission categories in 2015 were 40% for RWC, 31% for energy and heat plants and other stationary sources, 27% for vehicular traffic and 2% for harbors (Kaski et al., 2016; street dust not included in the inventory). Wood combustion is used as a supplementary heating method in ~90% of detached houses in the Helsinki metropolitan area. Aurela et al. (2015) discovered that during cold periods BBOA contribution to OA might be as high as 50% at the suburban residential sites.

Detailed monitoring of aerosol particle properties in urban and suburban areas is a challenging task due to fast fluctuating particle emissions and therefore, among other things, requires high time-resolution instruments. In addition to the continuous changes of emission sources, urban atmospheric aerosol is affected by weather, large scale movement of air masses, and on-going transformation of particles' physical and chemical properties strongly alters their concentration, size, and composition in time and space (e.g. Enroth et al., 2016; Heal et al., 2012; Birmili et al., 2013).

As a part of the MMEA Programme (Measurement, Monitoring and Environmental Assessment, 2010-2015, http://mmea.fi/mmea-program), a field campaign in winter 2012 was conducted in the Helsinki Metropolitan area, including measurements in the city centre, suburban densely populated small house areas with local wood burning as well as on major roads. Advanced on-line measurement techniques installed into a mobile laboratory van were used to monitor particle chemical composition, size distribution and volatility of fine particles. The objectives of this study were to explore the sources and characteristics of submicron particles in urban environments by investigating i) number and lung-deposited surface area concentration along with their size distribution, ii) BC, organic and inorganic composition of PM_1 mass, and iii) source components of organics by using positive matrix factorization (PMF). Furthermore, individual particle analyses with electron microscopy (TEM/EDX) were performed to obtain a comprehensive view on the properties and sources of typical particle types observed in the Helsinki metropolitan area in winter.

2. Experimental methods

2.1. Measurement sites

The mobile measurements were performed in the Helsinki metropolitan area on 15-27 February 2012. Two routes, one to east and the other to west from the city of Helsinki, were chosen such that they covered as diverse areas as possible; first on the busy streets in the Helsinki city centre (red line in Fig. 1), on the highways leading out from the city centre (black line), at suburban detached house areas (blue color), and at the urban background site on the shore of the Baltic Sea (black star). The annual mean traffic volumes were typically 10 000 - 40 000 and 40 000 – 80 000 vehicles per weekday for the city centre route and highway routes, respectively. Specific routes were planned for the measurements at six residential areas where many detached houses often use wood combustion for heating fireplaces and saunas (subplot in Fig. 1). The length of both routes was around 115 km, each of them was driven twice every other day at 5-10 pm. Furthermore, on 21 and 24 February measurements also occurred during the morning rush hours at 8-12 am. Two weekends 18-19 and 25-26 February were included in the campaign. The measurements were mainly performed in the evening periods to demonstrate the maximum impact of local RWC to air quality in the residential areas (Supplementary Fig. S1). The impact of local traffic emissions would have been even higher in the city centre and highways, if the measurement periods had been more focused on weekdays' rush hour times.

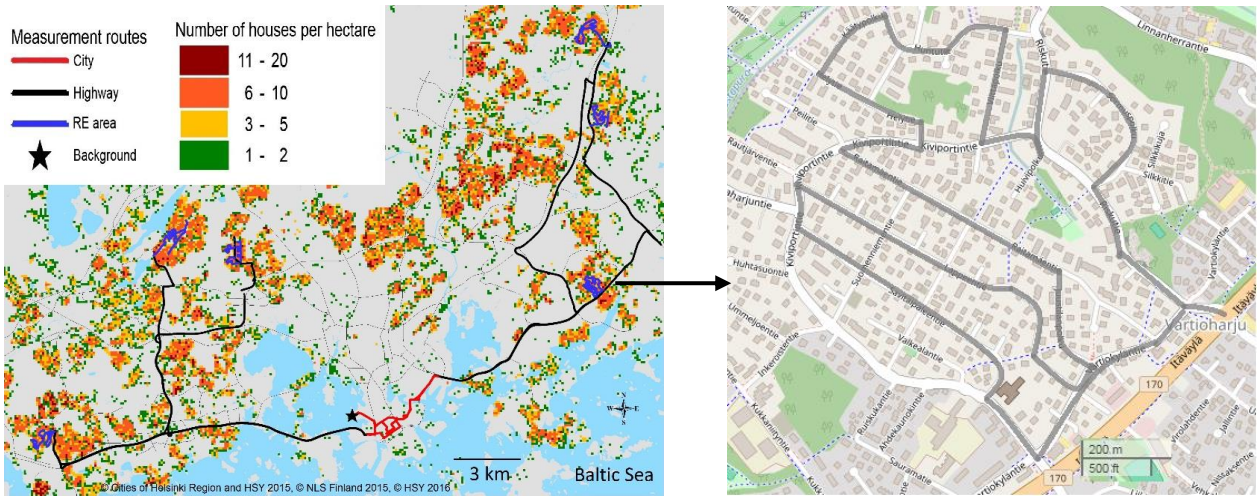

Fig. 1. The measurement routes and background site in the Helsinki metropolitan area. The density of detached and semidetached houses as well as the main road network are also shown for clarity. The subplot illustrates the driving route at an eastern residential small house area (Vartiokylä). (© OpenStreetMap contributors, CC BY-SA, see http://www.openstreetmap.org/).

2.2 Weather conditions

The weather was typical Finnish winter weather with permanent snow cover. During the campaign the temperature and relative humidity (RH), measured at the weather station Pasila at 30 m altitude above the sea level, varied from -7 ^{o}C to +1 ^{o}C, and from 64 to 85 %, respectively. The mean values with the standard deviations were -3 ± 2 ^{o}C and 80 ± 8 %, respectively (grey areas in Supplementary Fig. S2a). The long-term (1981-2010) mean values in February in Helsinki were -4.7 °C for temperature and 85% for RH (Pirinen et al., 2012). During a couple of days snowfall appeared preventing the measurements. The wind speed was 4.7 ± 2.4 m s^{-1} (Fig. S2b).

The 96 h backward trajectories calculated by the NOAA HYSPLIT model (Stein et al., 2015) showed that during the campaign air masses arrived in the Helsinki metropolitan area from four different directions; 1) on 15-19 February the air mass came from S/SE; 2) in the evenings of 20-21 February from NW, in the morning of 21 February from SW over the ocean carrying clean air; 3) on 24-25 February from NW but the air mass stagnated the last 21 hours above mid-Finland; however, on 25 February the air mass might capture air pollution from St. Petersburg about six hours before arriving Helsinki; 4) on 26-27 February directly from N (Fig. S3).

2.3. Instrumentation for mobile monitoring

Mobile monitoring was conducted with a mobile laboratory van "Sniffer" (VW LT35 diesel van) described in detail in Pirjola et al. (e.g. 2004; 2012; 2016) and Enroth et al. (2016). The sampling occurred at 2.4 m height from the ground level, above the van's windshield. Two separate inlet systems constructed of stainless steel were used; the instruments measuring the chemical properties of aerosol particles were connected to a sampling line with 8 mm inner diameter and 6 lpm flow rate, and the others to a sampling line with 20 mm inner diameter and 34 lpm flow rate. A list of the instruments is given in Supplementary Table S1.

Particle number concentrations and size distributions were measured with two ELPIs (Electrical Low Pressure Impactor, Dekati Ltd.) (Keskinen et al., 1992), one before and the other after a thermodenuder (TD) (Rönkkö et al., 2011). Both ELPIs were equipped with a filter stage (Marjamäki et al., 2002) and one ELPI with an additional stage designed to enhance the particle size resolution for nanoparticles (Yli-Ojanperä et al. 2010). The ELPI classifies particles in the size range of 7 nm – 10 µm (aerodynamic diameter) to 12 classes with one second time resolution. The cut-off diameters of the ELPI stages were 0.016 (additional stage), 0.030, 0.056, 0.093, 0.156, 0.264, 0.385, 0.617, 0.954, 1.610, 2.410, and 9.97 µm. The TD was used to study particle

volatility characteristics at the maximum operating temperature of 265 °C. Particle losses in the TD were corrected according to Heikkilä et al. (2009).

Lung deposited surface area (LDSA) concentration was measured by a nanoparticle surface area monitor (NSAM, TSI Inc., Model 3550) which collects particles electrically charged by corona type charger to a Faraday-cup type filter and uses an electrometer to measure the electrical charge carried by particles. The total LDSA concentration is calculated from the electric current as described by Fissan et al. (2007) and Asbach et al. (2009). To obtain the LDSA size distributions, the ELPI currents were multiplied by a factor of 60 $\mu m^2/(cm^3\ pA)$. More details of the determination of this calibration factor are presented by Kuuluvainen et al. (2016).

The Sniffer was also equipped with a SP-AMS (Soot Particle Aerosol Mass Spectrometer, Onasch et al., 2012) to futher study particle chemistry. In the SP-AMS, an intracavity Nd:YAG laser vaporizer (1064 nm) is added into the High Resolution Time-of-Flight Aerosol Mass Spectrometer (HR-ToF-AMS, DeCarlo et al., 2006) in order to measure refractory black carbon (rBC) and associated refractory particulate material (e.g. metals) in addition to the non-refractory species, sulphate (SO_4), nitrate (NO_3), ammonium (NH_4), chloride (Chl) and organics (Org). In this study the SP-AMS measured in mass spectrum (MS) mode with five seconds time resolution of which half of the time the chopper was open and half of the time closed. Every one minute the laser was switched on/off. The data shown in this paper for organics and inorganic species was measured only with the laser off. There was a PM_1 cyclone in front of the SP-AMS but the real measured size range of the instrument is ~70–500 nm with transmission efficiency of 100% (Canagaratna et al., 2007). The SP-AMS data was analyzed using a standard AMS data analysis software (SQUIRREL v1.57 and PIKA v1.16) within Igor Pro 6 (Wavemetrics, Lake Oswego, OR) and for the elemental analysis of organics an Improved-Ambient method was used (Canagaratna et al., 2015). The mass concentrations from the SP-AMS data were calculated by using a default collection efficiency of 0.5 (Canagaratna et al., 2007 and references therein). Default relative ionization efficiencies (RIE) were used for organics and inorganic species.

Black carbon (BC) in the PM_1 size fraction was measured by the one wavelength Aethalometer (Aethalometer, Andersen Instruments, RTAA 800) with a time resolution of 5 s. The aethalometer uses optical analysis to determine the mass concentration of black carbon particles collected from the air stream passing through a filter. The used optical wavelength is 880 nm in the IR range. Optical absorption is converted to the mass of BC and further to the mass concentration using a mass absorption cross section 16.6 $m^2\ g^{-1}$ (Arnott et al., 2005). The mass concentration was corrected for filter loading errors based on the procedure by Virkkula et al. (2007). The errors

resulted from a scattering of the filter material and particles cannot be corrected because no scattering measurement was available.

In this study, the PM_1 concentration was estimated as the sum of the concentrations of BC, measured with the aethalometer, and organics and inorganics measured with the SP-AMS. Gaseous concentrations of nitrogen oxides NO, NO_2 and NOx (model APNA 360, Horiba) were monitored above the windshield of Sniffer at the same altitude as particle concentrations with a time resolution of 1 s. A weather station on the roof of the van at a height of 2.9 m above the ground level provided meteorological parameters. Relative wind speed and direction were measured with an ultrasonic wind sensor (model WAS425AH, Vaisala); the temperature and relative humidity with temperature and humidity probes (model HMP45A, Vaisala). Additionally, a global positioning system (model GPS V, Garmin) recorded the van's speed and the driving route.

2.4. Positive matrix factorization

The organic aerosol fraction was investigated using Positive Matrix Factorization (Paatero, 1997) with PMF evaluation panel version 2.06 (Ulbrich *et al.*, 2009). The two input matrices consist of organic aerosol concentration in μg m^{-3} and respective uncertainties or errors. The rows of the matrices represent time series and the columns different variables (mass-to-charge ratios, m/z's). The number of factors in the dataset is unknown, and the final number of factors is defined by the user. The PMF method has been widely utilized in identifying multiple organic primary aerosol sources, i.e. traffic emissions, cooking and biomass burning, and in characterizing secondary organic aerosol (SOA) ageing factors (e.g. Lanz et al., 2010; Ulbrich et al., 2009; Zhang et al., 2011; Ng et al., 2011).

In this study before applying the final PMF analysis the AMS data were averaged to five minutes, as for five seconds time resolution no reasonable PMF results could be solved. Five minutes averaging time was still fast enough to get information of the different environments (city, highway, residential and background) in general. A three-factor solution was found to describe the sources of OA most reliably. The rotational ambiguity of the selected PMF solution and local minima were explored via the f-Peak parameter and seeds (Supplementary PMF Data Analysis). The factors were identified as HOA, OOA and BBOA, based on the reference mass spectra presented in the literature and by using auxiliary species such as BC, NO_x and/or inorganic ions. In a four-factor solution, the fourth factor had mainly features from the BBOA factor whereas in a

two-factor solution there was a separate HOA factor but OOA had some features from the BBOA factor.

In the three-factor solution, the HOA factor was dominated by ion series related to aliphatic or cyclic hydrocarbons (C_nH_{2n-1} and C_nH2_{n+1}) (Fig. S3), e.g. *m/z* 41, *m/z* 43, *m/z* 55, *m/z* 57, *m/z* 67, *m/z* 69, *m/z*, *m/z* 71, *m/z* 81, *m/z* 83 and *m/z* 85 (Zhang et al., 2005). HOA is typically emitted by combustion engines, such as from motor vehicles (Canagaratna et al., 2004). In this study HOA had the strongest correlation with other combustion-related components, e.g. NO_x (Pearson correlation coefficient r: 0.60) and BC (r: 0.56) indicating that HOA was mostly related to vehicle emissions. It also had very high correlation (r: 0.98) (Fig S5a) to mass spectra of HOA found in winter 2009 by Carbone et al. (2014).

OOA had very high contributions of *m/z* 44 and 28 (Fig. S3), which are mainly CO_2^+ and CO^+ ions, typically from the thermal decarboxylation of organic acid groups. The high contribution of these ions indicated highly oxidised OA. Multiple studies have shown OOA to be a surrogate for SOA, correlating well with secondary species (Zhang et al., 2005). In this study, the Pearson correlation coefficient between OOA and sulphate was 0.94, in agreement with a value of 0.99 (Fig. S5b) for OOA and LV-OOA presented by Carbone et al. (2014).

The third factor did not correlate well with any of the auxiliary species, but as the typical ions of BBOA, *m/z* 29 (CHO^+), *m/z* 60 ($C_2H_4O_2^+$) and *m/z* 73 ($C_3H_5O_2^+$) were present in this factor, it was assumed to be BBOA. These ions are associated with the fragmentation of levoglucosan and other anhydrous sugars (e.g. Alfarra et al., 2007). However, the overall contribution of m/z 60 was quite low in BBOA (Fig. S4) but was above the estimated background signal of m/z 60 from SOA (0.3%, Cubison et al., 2011). The Pearson correlation coefficient (r) of this factor with the biomass burning spectrum from Aiken et al. (2009), Mohr et al. (2012) and Carbone et al. (2014) were 0.92, 0.86 and 0.83, respectively (Fig S5c). Although in general BBOA did not correlate with BC, m/z 60 and BC had simultaneous concentration peaks during the RWC event (discussed in Section 3.2).

2.5. Individual particle analysis with TEM/EDX

The size-segregated particle samples (6 size fractions between 56 and 1 800 nm) for TEM/EDX were collected with a cascade impactor, using a Micro-Orifice Uniform Deposit Impactor with rotator (MOUDI™ Model 110-R, MSP Corporation, USA). During 15-min sampling periods for TEM/EDX, the mobile laboratory was parked. The sample collection with a volume flow rate of 30 liters per minute took place onto 3-mm TEM grids (Cu with carbon-coated Formvar films, 400-

mesh, Carbon Type-B, Ted Pella Inc., USA). The total number of TEM grids collected was 24, consisting of 4 sampling periods and 6 size fractions.

A transmission electron microscope (TEM; Tecnai 12, FEI Company, USA) equipped with an energy-dispersive X-ray micro-analyzer (EDX; EDAX Inc., USA) was used to analyze the following properties of individual particles; elemental composition, morphology and sensitivity to damage caused by an electron beam. The analysis procedure was the same as described in Niemi et al. (2006) and used also in other recent aerosol studies (Kerminen et al. 2011; Saarnio et al. 2014). The elements analyzed were from C to Pb, excluding N. Although the elemental results were semi-quantitative, the accuracy is sufficient to reliably identify different vacuum-resistant particle types (Niemi et al., 2006, and references therein). The high vacuum (10^{-7} Torr) and electron beam exposure cause evaporation of semi-volatile compounds from particles, and for that reason, water, ammonium nitrate and organic compounds with high-vapor pressure were lost, as is typical in electron microscopy. The smallest particles (~50-200 nm) with secondary components (e.g. ammonium, nitrate, sulphate and organics) are extra sensitive to beam damage and evaporation during individual particle EDX analysis occurs. The total number of individual particles analyzed was 1 129, typically ~50 particles per each TEM grid. The particle types and their classification criteria in this study is described in section 3.3.

2.6. Auxiliary measurements

The $PM_{2.5}$ mass concentration results of the official air quality monitoring stations in the Helsinki metropolitan area (Kaski et al., 2016) along with backward air mass trajectory analysis and chemical analysis of particle samples were used to obtain a general view on the local and LRT $PM_{2.5}$ levels during the research campaign (Figs. S3 and S6a). Furthermore, the levoglucosan concentrations were determined from daily PM_{10} samples collected at two suburban small house areas (Kattilalaakso and Vartiokylä; the most western and eastern RE areas in Fig. 1) and at an urban background site (Kallio) in the centre of Helsinki (Fig. S6b). The samples were collected with MicroPNS low volume (38 l min^{-1}) samplers on polytetrafluoroethylene filters, extracted with 5 ml of deionized water with an internal standard and analyzed with high performance anion exchange chromatograpy-mass spectrometry as described by Saarnio et al. (2012).

3 Results and discussion

311 *3.1. General overview - averages over the whole route*

312 During the campaign the route mean daily concentrations of particle number (Ntot) varied in
313 the range of (0.8-4.3)x10^4 cm^{-3} (Fig. 2a and Table 1); however, due to dynamic traffic conditions
314 the maximum one-second values were as high as 2.0x10^6 cm^{-3}. The lowest average concentrations
315 were observed on 18-19 and 26 February which were weekends. The average background particle
316 concentration, measured around 10 minutes by Sniffer at the urban background site, was 6x10^3
317 cm^{-3} or less except on 15, 18 and 25 February (Table 1 and Fig. S7a). The average Ntot
318 concentrations (Fig. 2a) nicely followed the NOx concentrations (Fig. 2b) indicating that most of
319 the Ntot emissions originated from traffic (Table 1).

320 The daily route average mass concentrations of PM_1, the sum of BC, organics and inorganics,
321 are shown in Fig. 2c and Table 1. During the first week with southern wind, the PM_1
322 concentrations (~20-60 μg m^{-3}) were clearly higher than during the rest of the campaign (~6-18 μg
323 m^{-3}) with the north-west wind as the prevailing wind direction. Particularly, on 15, 18 and 19
324 February, sulphate, ammonium, nitrate and organics concentrations were high, around 10 μg m^{-3},
325 3-4 μg m^{-3}, 2.8-4 μg m^{-3}, and 17-31 μg m^{-3}, respectively, due to high background concentrations
326 (Table 1 and Fig. S7b). Sulphate is typically long-range transported in Helsinki area (Aurela et al.,
327 2015). Based on the trajectory calculations (Fig. S3) in the evenings of 15, 18 and 19 February, the
328 origin of the airmass was from south/southeast from polluted areas in eastern Europe. During that
329 period, the elevated $PM_{2.5}$ concentrations (20-40 μg m^{-3}) were observed at all air quality stations in
330 the Helsinki metropolitan area, particularly, at the rural station (Luukki) and urban background
331 station (Kallio) as well as at the residential stations (Vartiokylä and Kattilalaakso) (Fig. S6a), and
332 the 24-h mean values were 28.4, 22.3 and 26.8 μg m^{-3} on 15, 18, and 19 February, respectively. In
333 general, atmospheric $PM_{2.5}$ concentrations are low in Finland due to low local emissions; the
334 annual mean values varied between 5 and 13 μg m^{-3} at different sites of the Helsinki metropolitan
335 area during years 2006-2015 (Kaski et al., 2016). All above mentioned facts indicate that long-
336 range transport (LRT) episodes occurred during these days. Furthermore, this conclusion is
337 supported by Niemi et al. (2009) who studied LRT episodes of fine particles in southern Finland
338 during 1999-2007, and discovered that at the urban background station Kallio the daily $PM_{2.5}$
339 mean exceeded 25 μg m^{-3} during 1-7 LRT episodes per year.

340 The $C_2H_4O_2^+$ ion (m/z 60), a tracer for biomass burning aerosol (e.g. Alfarra et al., 2007), also
341 showed elevated concentrations on 15, 18, and 19 February (Fig. S6b). The 24 h (daily) sampled
342 levoglucosan concentrations were high at the urban background station Kallio, and at two air

quality stations at the residential areas at Vartiokylä and Kattilalaakso (Fig. S6b), indicating that LRT aerosol contained also emissions from biomass burning.

The route average BC concentration was highest (9.9 ± 9.0 μg m^{-3}) on 15 February, for the other days it was smaller than 5 μg m^{-3}. The background BC concentrations were rather low, less than 1μg m^{-3} except on 24 February evening when it was 3.2 μg m^{-3} (Table 1).

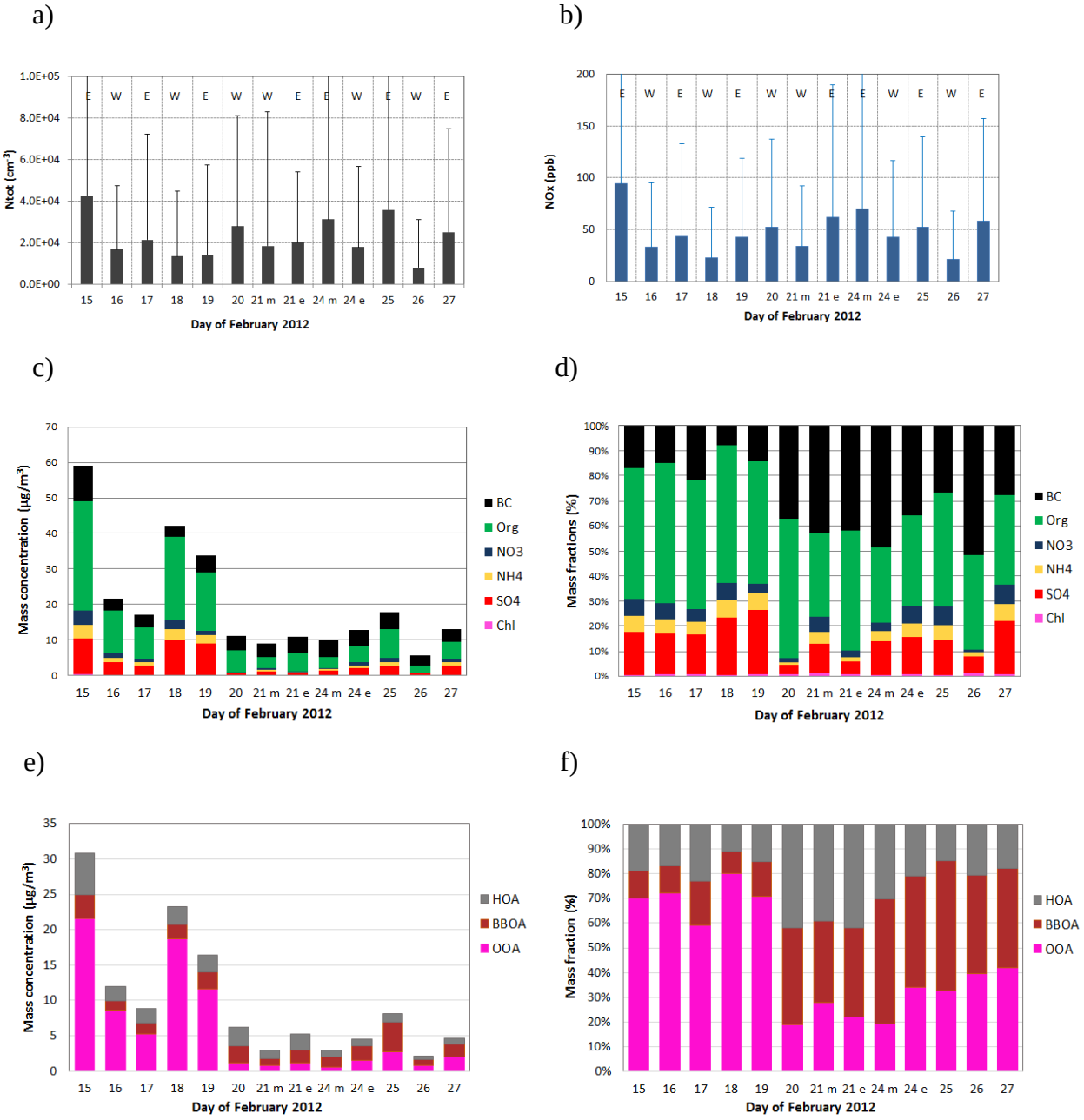

Fig. 2. Daily route averages of Ntot (a), NOx concentration (b), absolute and relative values of PM_1 chemical composition (c) and (d), and absolute and relative values of organic factors by PMF analysis (e) and (f). On 21 and 24 February the measurements were performed in the morning (m)

and evening (e), on the other days only in the evenings. E refers to eastern route, W to western route, and error bars to standard deviations. Background concentrations were not subtracted.

Table 1. Average pollutant concentrations over the whole route along with the average background concentrations measured by Sniffer.

Day of	Ntot (x 10^4 cm^{-3})		NOx (ppb)		BC (μg m^3)		Org (μg m^3)		Inorg (μg m^3)		PM_1 (μg m^3)	
February	route	bg	route	bg	route	bg	route	bg	route	bg	Route	bg
15	4.3	1.6	94.2	29.3	9.9	1.1	30.8	25.8	18.2	19.4	59.0	46.3
16	1.7	0.2	33.3	1.4	3.2	0.5	12.0	5.5	6.3	3.2	21.5	9.2
17	2.1	0.6	43.1	2.1	3.7	0.9	8.8	9.3	4.6	6.2	17.1	16.3
18	1.4	1.1	22.4	5.1	3.2	1.3	23.3	17.4	15.7	12.1	42.2	30.8
19	1.4	0.5	42.4	3.1	4.8	1.3	16.6	n.a.*	12.4	n..a.*	33.8	n.a.*
20	2.8	0.5	52.5	6.3	4.1	1.0	6.2	4.8	0.8	0.6	11.1	6.4
21 m	1.8	0.3	33.7	4.3	3.8	0.3	3.0	4.4	2.1	0.4	8.9	5.1
21 e	2.0	0.5	61.7	2.3	4.6	0.3	5.2	4.6	1.1	0.4	10.9	5.3
24 m	3.1	0.3	70.3	11.0	4.8	1.3	3.0	2.2	2.1	2.7	9.9	6.2
24 e	1.8	0.5	42.7	9.0	4.5	3.2	4.6	3.8	3.6	5.0	12.7	12.0
25	3.6	0.9	52.1	7.3	4.7	0.7	8.1	4.9	4.9	5.5	17.7	11.1
26	0.8	0.2	21.3	1.8	2.9	0.4	2.1	1.7	0.6	0.3	5.7	2.4
27	2.5	0.6	58.0	29.0	3.6	1.4	4.7	3.6	4.7	6.3	12.9	11.4

*data not available

Regarding the fractions of organic aerosol resolved by the PMF, OA consisted mostly of OOA during the south/south-east airmasses on 15-19 February. During the following days the fraction of OOA decreased significantly wheras the fractions of BBOA and HOA increased. In general, the route average contribution of OOA to organic aerosol varied between 19 and 80% (Fig. 2e,f). For HOA the contribution was highest on 20-24 February accounting for 39-42% of OA, while it had the lowest contribution to OA (11%) during the LRT episode on 18 February. The BBOA contribution varied between 11 and 52%, the highest contribution was observed on Saturday evening 25 February. During that evening the elevated contributions and concentrations of BBOA were mainly caused by local RWC since sauna stoves and other fireplaces are frequently used on Saturdays in Finnish culture. Furthermore, the accumulation of local emissions on 25 February might also enhancedue to very low wind speed (~1 m/s; Fig. S2).

Based on the molecular ratios of O, C and H, OOA was the most oxidized factor, whereas HOA was the least oxidized factor (Fig. S3). The OM:OC ratio for OOA, BBOA and HOA were 2.3, 1.6 and 1.3, respectively, which all of them were slightly higher than measured at the urban background site in Helsinki (Carbone et al., 2014). However, OM:OC, O:C and H:C ratios for

BBOA were very similar ton the local BBOA measured in Helsinki (Timonen et al.2013) whereas much higher OM:OC and O:C had been obtained for LRT BBOA (Timonen et al., 2013). This indicates that BBOA in our campaign was mainly from local sources, especially after the LRT episode.

With regard to PM_1, secondary components (OOA, NO_3, NH_4 and SO_4) dominated the PM_1 chemical composition on 15-19 February (LTR episode) accounting for 70-80% of the PM_1 mass, whereas fresh primary components (BC, HOA and BBOA) dominated on 21-26 February. BC and HOA constituted 56-62% of the total PM_1 on 20-24 and 26 February, largely due to traffic emissions.The route average BBOA fraction in PM_1 was 5-7% during the first five days, and 15-17% during the rest days of the campaign; however, on Saturday 25 February it increased up to 24% reaching a value of 4.3 $\mu g\ m^{-3}$.

3.2. Typical traffic, wood combustion, LRT and clean air features

In order to investigate the sources and characteristics of submicron particles in urban environments in more detail the measurement data were separated to city traffic (ci), highway traffic (hw), residential wood combustion (re) and background (bg) based on the areas where the measurements were carried out (Fig 1), and averaged accordingly. Four time periods were studied in detail; two Saturday evenings, one on 18 February during the LRT episode and the other on 25 February when the route average BBOA mass concentration was highest; two weekday mornings on 21 and 24 February when the background PM_1 concentrations were low but the HOA (traffic) contribution was clear.

The results are treated in three sub-sections. First, an example of the time series of the main pollutants are shown in section 3.2.1. Second, the average particle number and lung deposited surface area (LDSA) concentrations and size distributions are discussed in section 3.2.2. Thirdly, the average chemical mass compositions are considered in section 3.2.3.

3.2.1. Time series of main pollutants on 25 February

As an example, Fig. 3 illustrates the time series of the concentration of particle number (total number, number <30 nm particles and non-volatile particles), NO, NO_x, BC, organics, m/z 57 and m/z 60 on Saturday 25 February in the eastern route. The highest particle number and NO_x concentrations, $1.4x10^6\ cm^{-3}$ and 1.4 ppm, were measured on the highways. Volatile nucleation mode particles (< 30 nm in diameter) dominated the particle concentration on highways, whereas nucleation mode particles played a minor role on the residential areas. BC peaks were also

observed at the residential sites even though the highest momentary values up to 80 μg m^{-3} were measured on the highways. The elevated concentrations of organics and $C_2H_4O_2^+$ (m/z 60) at the residential sites re2, re3 and re1 after 7 pm (Fig. 3) indicated wood combustion emissions from smokestacks because the marker ion for traffic $C_4H_9^+$ (m/z 57) did not show simultaneous peaks.

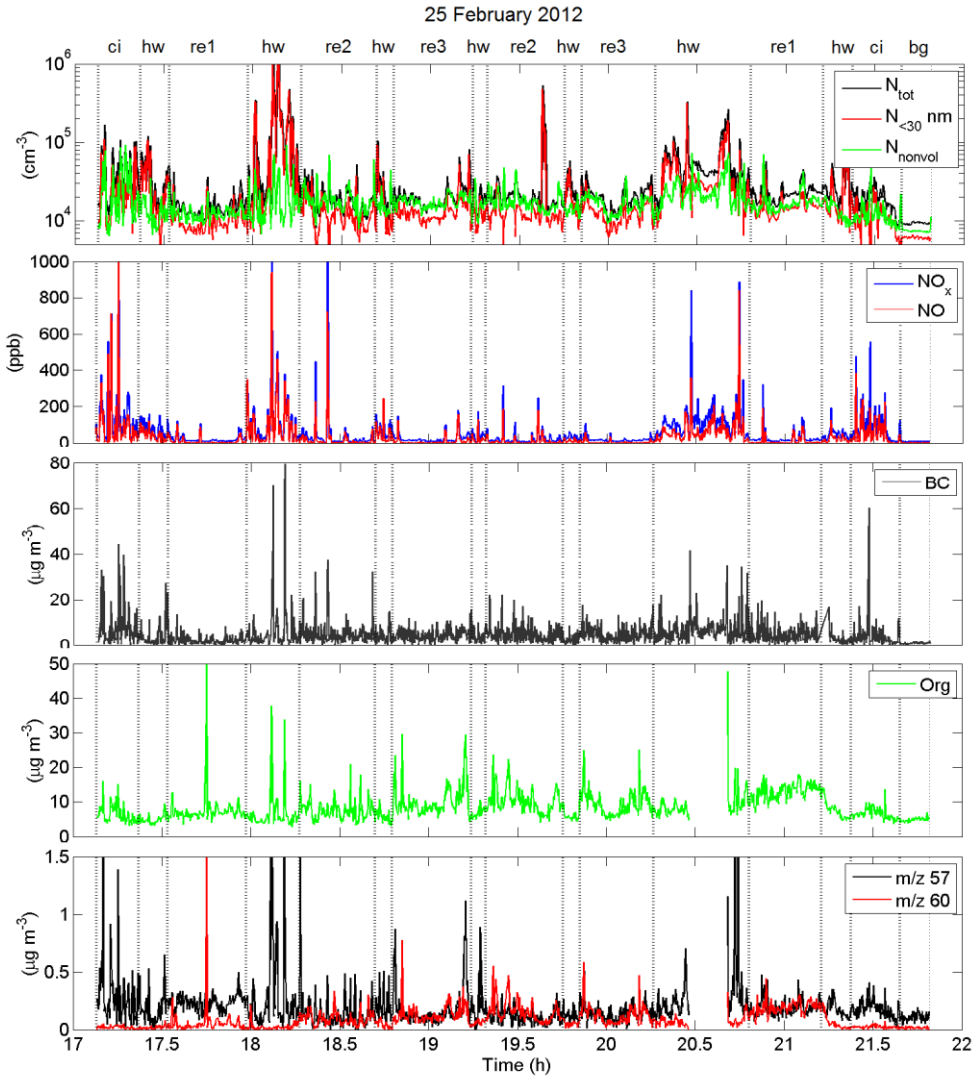

Fig. 3. Time series of the concentrations of all particles, nonvolatile particles, and particles smaller than 30 nm, nitrogen oxides, black carbon, organics as well as ions $C_4H_9^+$ (m/z 57) and $C_2H_4O_2^+$ (m/z 60), the tracers for traffic and biomass burning, respectively, on 25 February 2012.

3.2.2 Particle number and surface area concentrations and size distributions

Figure 4a illustrates the average concentrations of Ntot over the highways, city streets, residential areas and the background site for the four days (Table S2). Due to the fluctuating traffic

flow the concentration variation was high as seen from long errorbars, not only for one second values but also between the days. The Ntot was higher on the highways than on the city streets for all days. The source for these particles was traffic; however, on 18 February the relative portion of the background particles was high. At the residential areas local wood burning was the main source on Saturday 25 February because Ntot was around 2.5 times the background concentration and the vehicle traffic was minimal. For comparison, the average measured Ntot at the residential areas was 9-66% and 7-30% of those measured at the city and highway traffic, respectively.

The average total concentrations of the lung deposited surface area LDSA in different environments varied from 8 to 81 $\mu m^2\ cm^{-3}$ (Fig. 4b and Table S2). The lowest average concentration was measured in the background site on 21 February and the highest concentration on the highway on 25 February.

a) b)

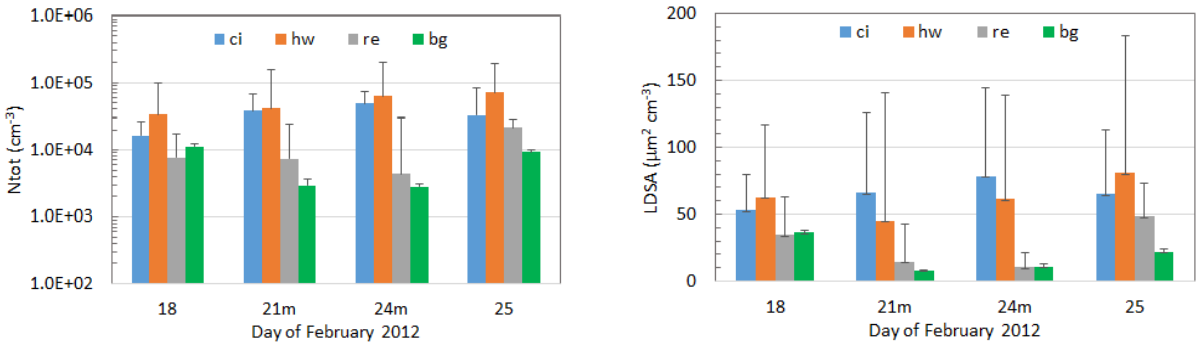

Fig. 4. Average concentrations of particle number Ntot (a) and lung-deposited surface area LDSA (b). Error bars refer to the standard deviations of the measured 1 s values in each environment mentioned in the legend.

Particle number size distributions (Fig. 5a) at the traffic environments possessed two modes as typical for car exhaust particles (e.g. Kittelson, 1998; Hussein et al., 2005; Kumar et al., 2008; Pirjola et al., 2012; Enroth et al., 2016); a nucleation mode peaked at 10-20 nm and a soot mode at ~ 75 nm. Stop-and-go driving in the city centre leads to several accelerations and consequently, the soot mode is emphasized for the city traffic particles, whereas the nucleation mode is larger for the highway particles. Additonally, on 18 February during the LRT-episode a third mode peaking at around 300 nm (aerodynamic diameter) can be distinguished. The origin of this mode is from the background particles. The volatility measurements showed that 57-68 % and 73-80% of the particles by number in the city and on the highways, respectively, evoporated at the thermal

treatment. Most of them were in the nucleation mode (< 40 nm diameter) indicating that the origin for these particles might be nucleation of sulfuric acid from fuel and lubricant oil sulfur compounds along with volatile organic compounds (Arnold et al., 2012, Kittelson et al., 2008; Tobias et al., 2001; Schneider et al., 2005). The existence of non-volatile cores (e.g., Rönkkö et al., 2007) in sub 30 nm particles could not be estimated because particles smaller than 7 nm cannot be measured by the ELPIs. Similar results from other mobile measurements have been published. Pirjola et al. (2012) report that during morning rush hour in the Helsinki city centre the average particle concentration was (5.1±3)x10^4 cm^{-3}, the particles possessed two modes peaking at 10-20 nm and 70-80 nm, and around 75-80% of particles by number was volatile, whereas Enroth et al. (2016) measured exhaust particles on the highways in the Helsinki metropolitan area during rush hour, and report somewhat higher average particle concentrations (7.7-12.3)x10^4 cm^{-3}, of which around 86% by number were observed to be volatile. These results are also in agreement with the measurements in an Alpine valley by Weimer et al. (2009) who discovered on the highway that more than 80% of the particles consisted of volatile components and the predominat particle sizes were in the nucleation mode. At the residential areas, the size distributions were bimodal as well but the concentrations were smaller, and the accumulation modes were wider than in the city streets and on highways.

a)

b)

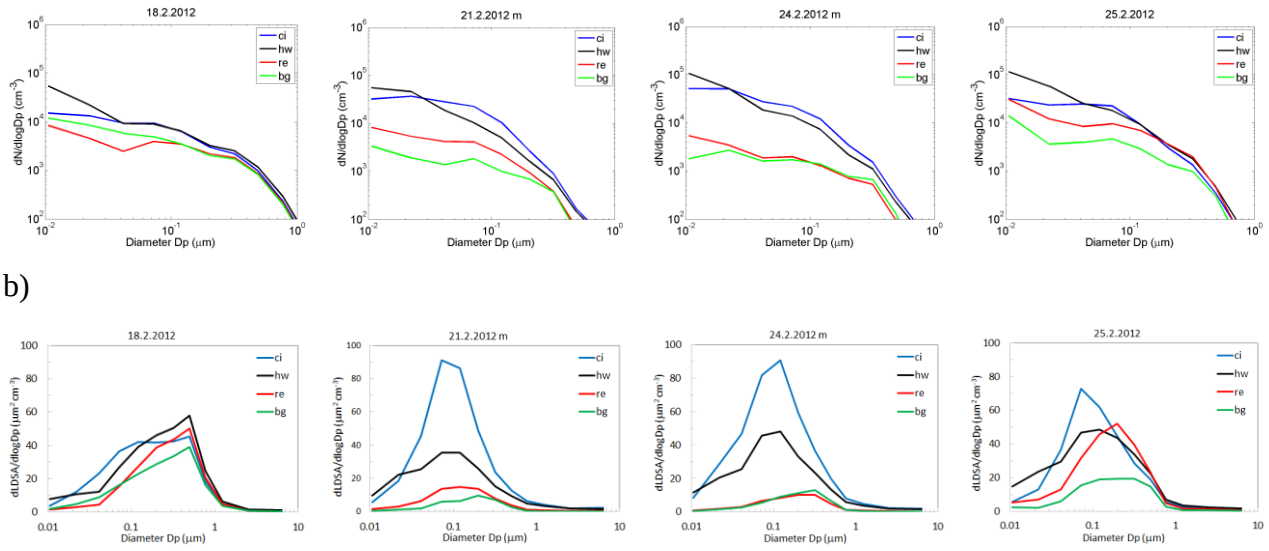

Fig. 5. Average particle number (a) and lung-deposited surface area size distributions (b) in different environments for the four days.

Furthermore, lung deposited surface area (LSDA) size distributions are presented in Fig. 5b. The soot mode peaking at ~100 nm dominated the size distribution in the city, whereas the nucleation mode also had a clear contribution particularly on the highways, the mode typically peaked at 20-25 nm. The backgound particles played a minor role besides on 18 February due to the LRT-episode, when in addition of the nucleation and soot mode a third mode peaking at ~500 nm could be distinguished. Sillanpää et al. (2005) studied mass size distributions in Helsinki and discovered a large accumulation mode peaking at 510 nm (aerodynamic diameter) during LRT smoke episodes. Although the total LDSAs were higher in the traffic environments, wood burning dominated the average LSDA size distribution in the residential areas on 25 February, the mode peaked at 200 nm and was higher than the accumulation mode in the highway environment. This is plausible, since particles in the residential area were more aged and oxidized than fresh emissions measured by Sniffer on the higway. In addition, the surface area concentration of the nucleation mode particles was much lower in the residential areas compared to the city and highway environments. The average LSDA value and size distribution over all campaign days in different environments are presented in Kuuluvainen et al. (2016).

3.2.3 BC and organic composition

The PM_1 chemical composition and organic factors in different environments are presented in Fig. 6 for the selected days. The average BC concentration was larger in the city than on the highway, and in both environments larger than at the residential areas (Table S2). Of PM_1 mass black carbon accounted for 7-12% on 18 February, whereas on 21 and 24 the percent was between 40 and 50 (Table S3). However, in the background site the percent was much lower 4-6%, except 19% on 24 February. On average over the four days, organic aerosol accounted for 43±8, 39±11, 43±15, and 40±19% of PM_1 mass in the city, highway, residential and urban background environments, respectively (Table S3). The highest OA percents of PM_1, 54-55% in the traffic, and 58-59% in the residential and background sites, were obtained on 18 February during the LRT episode. Inorganic species had the highest contribution to the background aerosol, they accounted for 41±5% of the PM_1 mass with a small variation between the days. However, on 21 February when very clean airmass arrived over the ocean, the inorganics accounted only ~8% of PM_1 mass. In the traffic and residential environments the contribution of inorganics was on average 12-28%, but in the LRT episode day it was larger being 33-36%. This showed that the main sources of inorganics were not in traffic or residential areas. Sulphate was the dominant inorganic species followed by nitrate and ammonium. Chloride had a notable contribution to the composition on 21

February probably due to sea salt from the ocean and the use of de-icers on roads to prevent slipperiness.

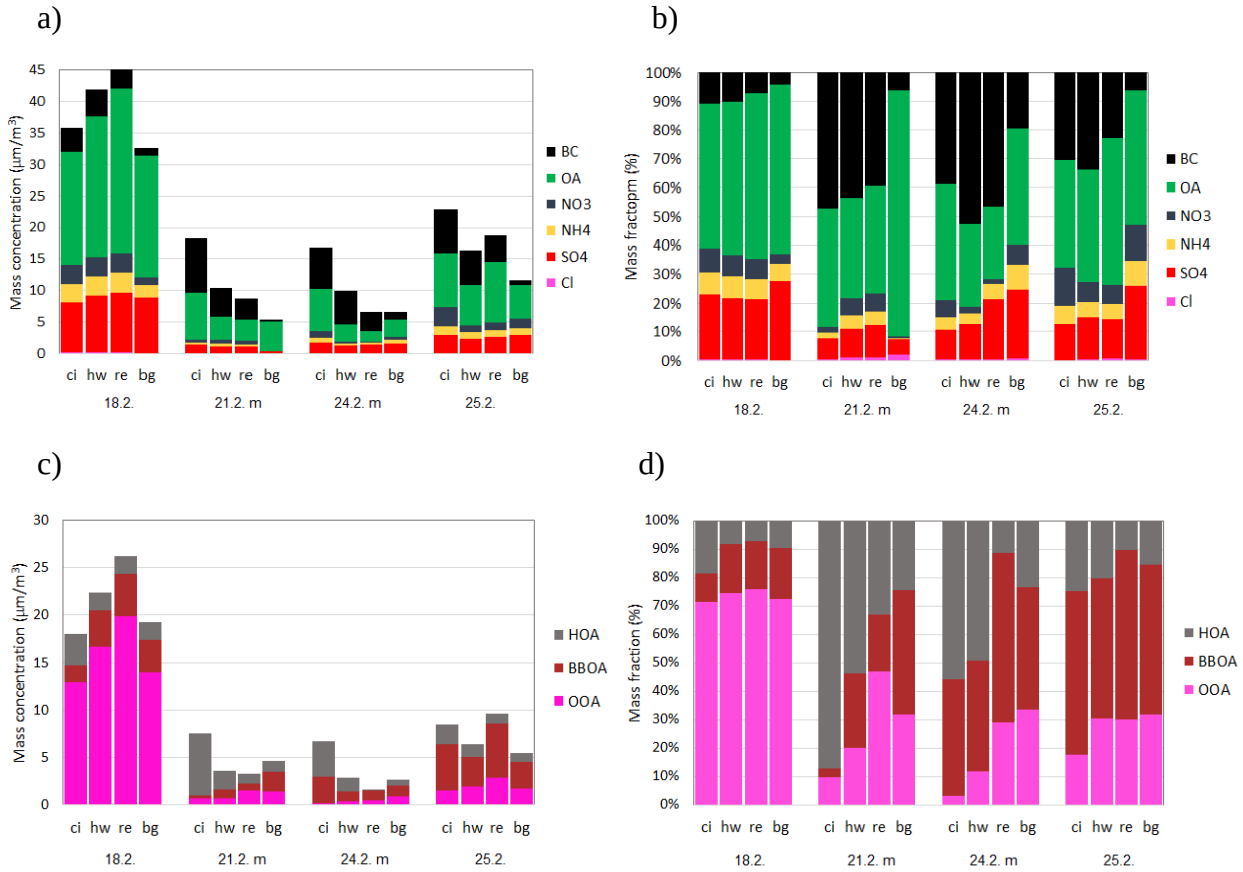

Fig. 6. Average mass concentrations of PM_1 chemical composition (a), and organic factors (c) in different environments for the selected days. Also shown are mass fractions of organic (b) and PM_1 components (d).

According to the source apportionment of organic aerosols (Fig. 6c,d), the contribution of HOA to OA was largest in the city followed by the highway, similar to BC. Highest HOA contributions were measured on 21 and 24 February accounting for 87% and 56% of OA in the city, and 54% and 49% of OA on the highway, respectively (Table S3). During those days the contribution of background aerosol to the measured concentrations was very small, the PM_1 mass of the background particles was low, 5.4 and 6.7 µg m^{-3}, respectively (Table S2). The BBOA had the highest contribution to OA on 24 - 25 February in the residential areas accounting for 59-60% of OA, close to the highest values reported by Aurela et al. (2016). In Helsinki, the contribution of wood burning to the concentrations of organic carbon has been ~40% in winter 2006-2007 (Saarikoski et al., 2008), but much less in 2009 ranging between 1 and 39 % (Carbone et al.,

2014). Regarding OOA it had highest contribution (71-76%) during the LRT episode day independently of the environment, whereas on the other days it was typically ~30% in the residential and background sites, and lowest (< 20%) in the traffic sites on 21 and 24 February.

3.3. Individual particle analysis

The individual particle TEM/EDX analysis was performed for the four samples collected on three days. Different from the continuous online measurements discussed above, 15 minutes TEM/EDX samples were "snapshots" of typical aerosol types in the Helsinki metropolitan area in winter (Table S4); 1) city center kerbside site during Friday morning rush hour characterized with emissions from local traffic (TRAFFIC; PM_1 concentration ~12 μg m^{-3}), 2) suburban small house area site during Saturday evening characterized by emissions from local residential wood combustion in fireplaces (RWC; PM_1 ~43 μg m^{-3}) and simultaneous LRT pollution episode, 3) urban background site during strong LRT pollution episode (LRT-EPI; PM_1 ~31 μg m^{-3}) due to air flowing from the polluted areas of eastern Europe, and 4) urban background site during very clean period (CLEAN; PM_1 concentration ~5 μg m^{-3}) due to marine air flowing from the Atlantic Ocean. In regard to the four days discussed in previous section, the four TEM/EDX samples were collected in three of those days (18, 21 and 24 February).

The individual particles analysed with TEM/EDX were classified into 10 particle types based on their elemental composition (elements with atomic number Z from C to Pb, excluding N), morphology and susceptibility to damage by an electron beam; 1) soot, 2) tar ball, 3) C-rich, 4) K/S/C-rich, 5) S with V-Fe-Ni, 6) S/C-rich, 7) Na/Cl-rich, 8) Ca-rich, 9) Si/Al-rich, and 10) transition metals (Table S4).

The abundances of individual particles types varied significantly in the four different aerosols (Fig. 7). As expected, the highest proportion (~100%) of soot particles was observed in the 56-180 nm size range of the kerbside aerosol (TRAFFIC), since black carbon is the major component of fresh exhaust particles in that size fraction (Enroth et al. 2016). The fractal-like nanoparticle chains and chain-agglomerates of these fresh soot particles (Fig. 8a) were not yet collapsed or coated with heavy layers of secondary components, as often observed in aged and long-range transported soot particles (LRT-EPI and CLEAN; Fig. 8d; Niemi et al. 2006). The fresh soot particles from traffic were mainly composed of C and minor O, while many soot particles from local residential wood combustion aerosols (RWC) also contained detectable amounts of K and S that are typical elements in wood combustion emissions (Torvela et al. 2014).

Tar balls are individual spherical C-rich particles that are dark (electron-dense), amorphous and totally stable even in the presence of very strong electron beam (Fig. 8c). They originate from biomass burning (e.g. Pósfai et al. 2004; Martinsson et al. 2015), and they are a main source of organic light-absorbing brown carbon (BrC) in the atmosphere, resulting in significant climate-warming impacts (Alexander et al. 2008; Hoffer et al. 2016; Liu et al. 2016). In this study, tar balls were observed in every size fraction (56-1800 nm) but their amounts were quite small in most samples (Fig. 7). The highest proportions (average 5% in the 56-1000 nm size range) were observed during the LRT episode, when polluted air masses from eastern Europe also carried significant amounts of particles from wood combustion (Figs. S6, 2 and 6). This 5% proportion is higher than observed during a LRT pollution episode in Finland in spring 2004 (1-2% in the 200-1000 nm size range; Niemi et al. 2006), but much lower than at K-puszta regional background site in Hungary in cool season samples (~10-40%; Pósfai et al. 2004) and in the smoke plumes of open biomass burning fires (maximum even >80%; Pósfai et al. 2004, Hand et al. 2005). The elemental composition of the tar balls was similar as observed in the previous studies; abundant C, some O and sometimes also minor amounts of other elements, such as K and/or S (e.g. Pósfai et al 2004; Hand et al. 2005; Niemi et al. 2006; Adachi and Buseck 2011). The RWC sample contained abundant K/S/C-rich particles and some soot particles, indicating that they mainly originated from quite high-quality or flaming combustion conditions (Martinsson et al. 2015; Torvela et al. 2014). This kind of conditions are not favourable for tar ball formations since they are mainly formed in poor combustion conditions, such as low temperature pyrolysis during wood addition to fireplace (Martinsson et al. 2015), smoldering burning conditions and wildfires (Pósfai et al 2004; Hand et al. 2005; Adachi and Buseck 2011).

C-rich particles that were not soot particles or tar balls were also observed (Figs. 7 and 8b). This C-rich group contained particles with highly variably morphology and sensitivity to beam damage. In addition to C, these particles contained some O and sometimes minor S, K and/or Si. C-rich particles were observed in every size fraction (56-1800 nm) but their amounts were usually quite small. The highest proportion (36%) of C-rich particles was observed in the 560-1000 nm size fraction of the RWC sample, and they probably originated from the local emissions of wood combustion (Fig. 8b). In general, the source of C-rich particles remained uncertain, but during winter they might mainly be emitted from various combustion sources. Few C-rich particles might also originate from natural sources (Niemi et al. 2006) since high concentrations of fluorescent particles were observed during the LRT episode (Saari et al. 2015).

K/S/C-rich particles were enriched in the RWC aerosol and their proportions were 69-75% in the size fractions between 56-320 nm (Fig. 7), indicating clearly typical chemical components (K, sulphate, organics) from wood combustion (Torvela et al 2014). The morphology of particles was highly variable (Fig. 8b). Many of these particles contained also minor amounts of Zn, which often acts as a condensation nuclei in cooling wood combustion emissions (Torvela et al. 2014). Based on the recent study by Uski et al. (2015), ZnO may be a key component producing toxicological responses in the PM emissions from very efficient wood combustion. K/S/C-rich particles with beam-sensitive secondary components were also detected in all aerosols studied, emphasizing that the wood combustion and/or other biofuel emissions were always present in regionally and long-range transported winter aerosols (Figs. 2 and S6). The emissions from diesel vehicles might also be a potential source for some K/S-rich particles (Karjalainen et al., 2016; Rönkkö et al., 2014).

Particles of the S/C-rich group were usually very sensitive to beam-damage since they mainly contained secondary aerosol components, e.g. sulphate and organics. The S/C-rich particles were sometimes internally mixed with soot particles or other beam-resistant inclusions such as minor amounts of K (Fig. 8c-d). S/C-rich particles are typically observed in regionally and long-range transported aged aerosols (e.g. Niemi et al. 2006; Kerminen et al. 2011). Therefore, this particle type was very common in all aerosols studied (Fig. 7), especially when the contribution of local emissions sources was low compared with background level caused by regional and LRT aerosols (LRT-EPI and CLEAN). A few of S-rich particles contained also V, Ni and Fe (Fig. 8c). These particles were only present in the smallest size fractions (56-320 nm; Fig. 7), suggesting that they might originate from nearby sources, for example from heavy fuel oil combustion, in heat plants and ships (Happonen et al., 2013).

The shares of Na/Cl-rich particles were highest in the 560-1800 nm size range of the CLEAN aerosol (Figs. 7 and 8d) due to sea salt, since the air flows arrived from the Atlantic Ocean and via the Baltic Sea. The amount of Cl was usually very low, as typical for LRT sea salt, due to reactions with gaseous pollutants (e.g. Niemi et al., 2005; 2006). In the TRAFFIC sample, Na/Cl-rich particles might also partly originate from de-icer street salt (NaCl), since the ratio between Na and Mg-Ca-K deviated from the typical composition of sea salt. The TRAFFIC sample also contained highest proportions of Si/Al-rich particles (Figs. 7 and 8a) that probably originated from asphalt wear caused by studded tyres and antiskid sanding materials (Kupiainen et al., 2016).

In transition metals group, almost all particle were mainly composed of Fe and O, but few particles were also enriched with other transition metals, such as Zn, Mn and/or Cr. The highest

proportion (24%, Fig. 7) of Fe-rich particles was in the 1000-1800 nm size faction of the TRAFFIC aerosol and their shapes were mainly angular (Figs. 7 and 8a). Thus, the Fe-rich particles of that sample might mainly originate from the wear products of brakes as well as from tram wheels and trails near the sampling site. Only few of the transition metal (and Si/Al-rich) particles were circular, indicating that most of them were not released from high-temperature combustion conditions, such as coal-fired power plants or metal industry (Saarnio et al. 2014). In general, transition metals may originate from several anthropogenic sources (Lin et al. 2015; Jeong et al. 2016), and their identification was beyond the scope of this study. Few Ca-rich particles were observed in all samples (Fig. 7), and potential sources for them include emissions from coal combustion and their desulphurization products, wood combustion, road dust, cement and metal industries and even marine origin (Saarnio et al. 2014; Niemi et al. 2006 and references therein).

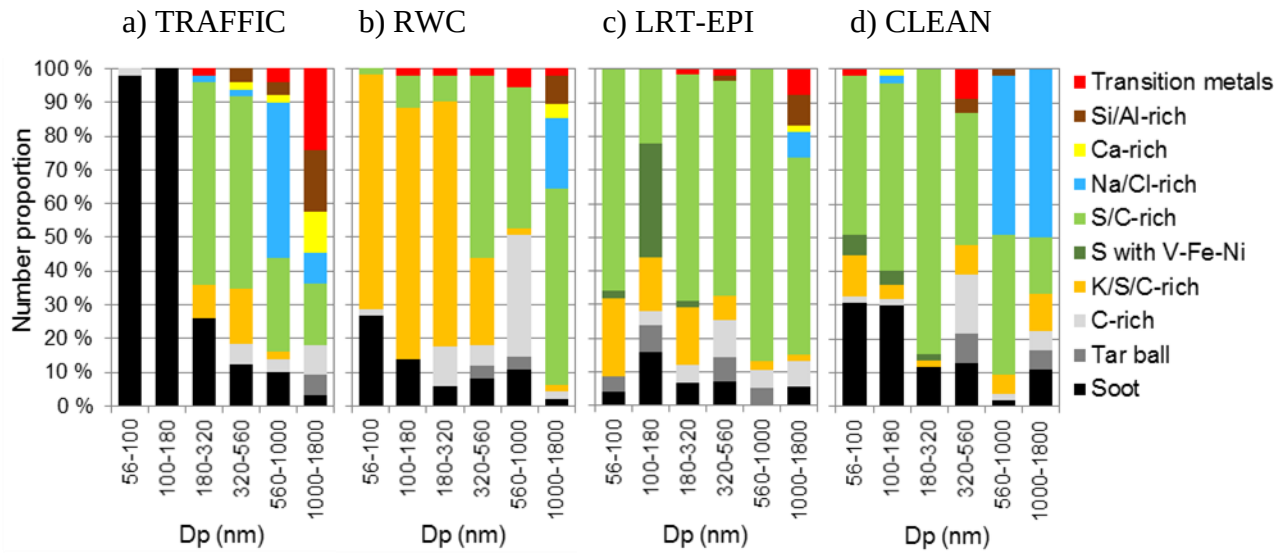

Fig 7. Relative abundances of particle types in different size fractions for the four studied winter aerosols characterized mainly by emissions from local traffic (a), emissions from local residential wood combustion mixed with LRT pollution episode (b), LRT pollution episode (c), and very low urban background PM during clean marine period.

4 a) TRAFFIC b) RWC

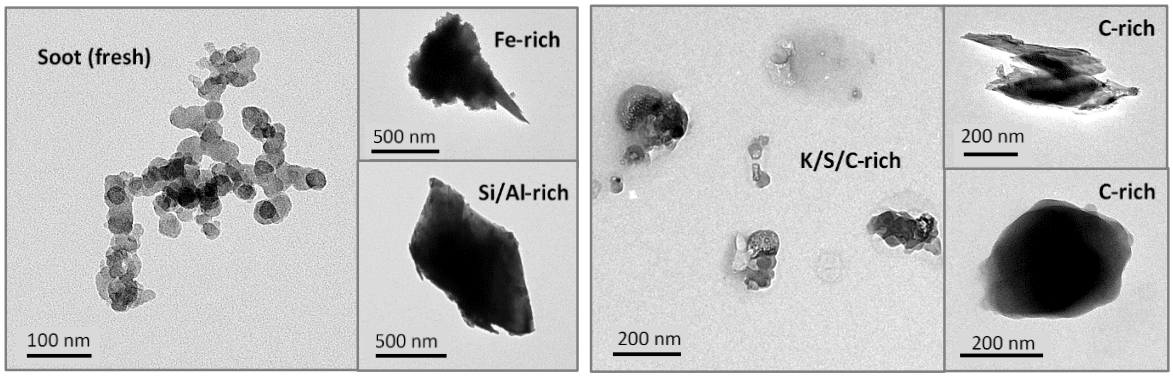

d) LRT-EPI e) CLEAN

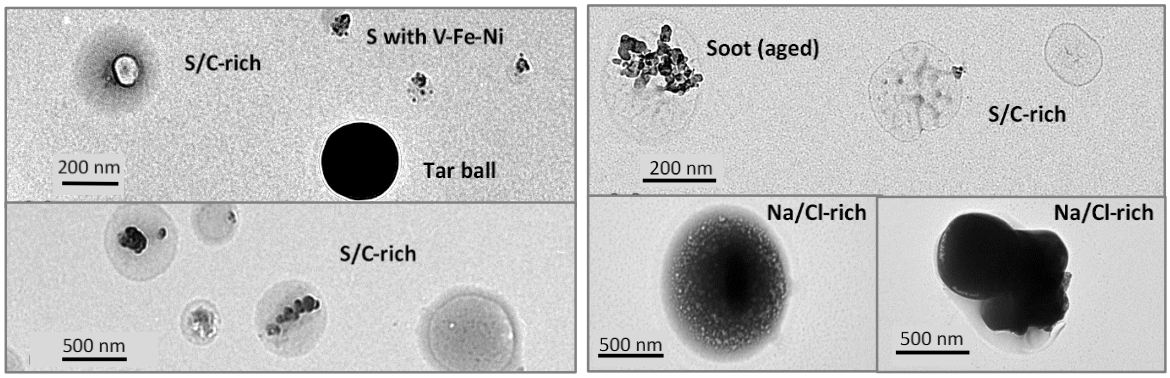

Fig. 8. TEM images of typical individual particle types observed in the four studied winter aerosols.

8 Conclusions

A field campaign in the city and densely populated small house areas with local wood burning as well as on major roads was conducted by the mobile laboratory van Sniffer in the Helsinki metropolitan area on 15-27 February 2012. The installed state-of-the-art instrumentation with 1-5 s time resolution enabled us to obtain a comprehensive view on aerosol properties and sources. Based on the trajectories and identified organic factors, namely OOA, BBOB, HOA, by PMF analysis, four major types of winter aerosol were recognized:

- clean aerosol at urban background site on seashore due to marine air flows from the Atlantic Ocean (21 Feb)
- LRT pollution episode aerosol due to air flows from eastern Europe with high OOA (18 Feb)

- local traffic related aerosol from fresh traffic emissions (HOA) while driving on busy streets in the Helsinki city centre and on the highways during morning rush hours (21 and 24 Feb)
- local residential wood combustion related aerosol from fresh smoke plumes (BBOA) in suburban small house areas (25 Feb).

Meteorology played a major role in the two first types. The average PM_1 concentration was much higher, 32.6 μg cm^{-3}, for the LRT emissions than for the local average RWC (18.8 μg cm^{-3}) and traffic (13.9 μg cm^{-3}) emissions (Fig. S8a). Fig. S8a,b also shows that secondary components (OOA, NO_3, NH_4, and SO_4) dominated the PM_1 chemical composition during the LRT episodes accounting for 70-80% of the PM_1 mass, whereas fresh primary emissions (BC, HOA and BBOA) dominated PM_1 during the local emissions (60-80%). However, the effects of the primary emissions from the Helsinki metropolitan area on local air quality are less significant than the effects of LRT emissions. Similar results have been reported e.g. Grippa et al., (2013) for the Paris megacity. In regard to particle numbers, traffic emissions played a major role (Fig. S8c).

Clean background aerosol was characterized by low number, LDSA and BC concentrations, (3.0±0.7)x10^3 cm^{-3}, 8.0±0.4 μm^2 cm^{-3}, and 0.3±0.2 μg m^{-3}, respectively (Table S2). OA dominated the low PM_1 mass concentration (~5.4 μg m^{-3}).

For the traffic related aerosol, the particle number size distribution possessed two modes, the nucleation mode peaked at 10-20 nm and the soot mode at ~75 nm (aerodynamic diameter). Sometimes a third mode peaking at around 300 nm (aerodynamic diameter) was observed as well, but it orginated from the background aerosol. Due to the stronger nucleation mode the average total particle number concentration was higher on the highways (6.3±11.7)x10^4 cm^{-3} than on the city streets (4.8±5.1)x10^4 cm^{-3}. Instead, the soot mode concentration was higher for the city particles due to stop-and-go driving resulting in the higher lung deposited surface area (78±66 vs. 62±78 μm^2 cm^{-3}) and BC concentrations (6.6±8.0 vs. 5.2±8.6 μg m-3) compared to the highway particles. On average, the PM_1 mass of the traffic environments comprised 39-53% of BC, 29-40% of OA and 12-22% of inorganic species (Table S3). HOA had the highest contribution to OA (49-87%) followed by BBOA (3-39%) and OOA (3-12%).

In the residential areas, lower number concentration ((2.1 ±2.4)x10^4 cm^{-3}) and larger particles in the soot mode (LDSA = 49±24 μm^2 cm^{-3}) characterized the physical properties of the smoke particles. The chemical composition was dominated by organic material. On average, the PM_1

comprised ~51% of OA, ~26% of inorganic species, and ~23% of BC. BBOA had the highest contribution to OA (59%) followed by OOA (30%) and HOA (10%).

During the LRT episode, organic aerosol dominated the PM_1 chemical composition independently of the environment accounting for 54-59% of the mass. The average contribution of OOA to OA was overpoweringly the largest 71-76%, BBOA and HOA contributed much less, each of them around 10-18%. The inorganic species, mainly sulphate, comprised 33-37% of the PM_1, instead the BC had only minor effect 4-7%, except 10-12% in the traffic environments. The average background particle number and LDSA concentrations were rather high $(1.1\pm0.1)\times10^4$ cm^{-3} and 36 ± 2 μm^2 cm^{-3}, respectively, compared to other winter aerosol types.

Furthermore, the four typical aerosol types in the Helsinki metropolitan area in winter were analyzed with transmission electron microscopy (TEM/EDX). In the small house area during Saturday night, the aerosols were enriched with emissions from local residential wood combustion in fireplaces, resulting in high amounts of K/S/C-rich, soot and other C-rich particles. In the city center kerbside during morning rush hour, particles in the 56-180 size range were strongly dominated (~100%) by fresh soot particles and also minor amounts of non-exhaust emission of traffic were present (Si/Al-rich, Fe-rich) in the larger particle sizes.

In the urban background site, aerosols contained abundant S/C-rich secondary particles, especially during the LRT episode from eastern Europe. Minor amounts of tar balls, i.e. brown carbon containing spherical C-rich particles from wood combustion, were observed in the all four aerosols studied and their proportions were highest (~5%) during the LRT pollution episode. A few particles with S and V-Ni-Fe were also detected, originated e.g. from the emissions of heavy oil combustion in heat plants or ships. The proportion of Na/Cl-rich sea salt was highest during very clean period at background site, since air flows arrived to Helsinki from the direction of the Atlantic Ocean.

In conclusion, the mobile online measurements of aerosols showed that the compositions, size distributions and sources of fine particles are highly variable in time and space in the Helsinki region in winter. Furthermore, the TEM/EDX analysis of selected aerosols provided detailed information on different individual particle types, including their elemental characteristics, morphology and mixing state, thus complementing the results of online methods. A comprehensive view of aerosol properties and sources in urban air is important for air quality assessment, in characterizing human exposure, and for climate models. For the use of epidemiological studies and exposure estimation, it is important to know LDSA concentrations and size distributions at different populated areas.

Acknowledements

The MMEA project was supported by Tekes **(**the Finnish Funding Agency for Technology and Innovation) and coordinated by the Finnish energy and environment cluster - CLEEN Ltd. The authors are very grateful to Aleksi Malinen, Kaapo Lindholm and Taneli Fabritius from the Metropolia University of Applied Sciences for technical expertise and operation of Sniffer. We also thank Karri Saarnio from Finnish Meteorological Institute as well as Sampo Saari and Anssi Järvinen from Tampere University of Technology for their contribution to the measurements. The authors gratefully acknowledge the NOAA Air Resources Laboratory (ARL) for the provision of the HYSPLIT transport and dispersion model and/or READY website (http://www.ready.noaa.gov) used in this publication.

Appendix A. Supplementary data

748 **References**

749 Adachi, K., Buseck, P.R., 2011. Atmospheric tar balls from biomass burning in Mexico. Journal
750 of Geophysical Research 116, D05204, doi:10.1029/2010JD015102
751 Aiken, A. C., Salcedo, D., Cubison, M. J., Huffman, J. A., DeCarlo, P. F., Ulbrich, I. M.,
752 Docherty, K. S., Sueper, D., Kimmel, J. R., Worsnop, D. R., Trimborn, A., Northway, M.,
753 Stone, E. A., Schauer, J. J., Volkamer, R. M., Fortner, E., de Foy, B., Wang, J., Laskin, A.,
754 Shutthanandan, V., Zheng, J., Zhang, R., Gaffney, J., Marley, N. A., Paredes-Miranda, G.,
755 Arnott,W. P., Molina, L. T., Sosa, G., Jimenez, J. L., 2009. Mexico City aerosol analysis
756 during MILAGRO using high resolution aerosol mass spectrometry at the urban supersite (T0)
757 – Part 1: Fine particle composition and organic source apportionment. Atmos. Chem. Phys. 9,
758 6633– 6653.
759 Alexander, D. T. L., Crozier, P. A., Anderson, J. R., 2008. Brown carbon spheres in Ease Asian
760 outflow and their optical properties. Science 321, 833-836.
761 Alfarra M.R., Prévôt A.S.H., Szidat S., Sandradewi J., Weimer S., Lanz V.A., Schreiber D., Mohr
762 M., Baltensperger U., 2007. Identification of the mass spectral signature of organic aerosols
763 from wood burning emissions. Environ. Sci. Technol. 41, 5770–5777.
764 Alföldy, B., Gieschaskiel, B., Hofmann, W., and Drossinos, Y.: Size-distribution dependent lung
765 deposition of diesel exhaust particles, J. Aerosol Sci. 40, 652-663, 2009.
766 AMAP, 2011. The Impact of Black Carbon on Arctic Climate (2011). By: P.K. Quinn, A. Stohl,
767 A. Arneth, T. Berntsen, J. F. Burkhart, J. Christensen, M. Flanner, K. Kupiainen, H.
768 Lihavainen, M. Shepherd, V. Shevchenko, H. Skov, and V. Vestreng. Arctic Monitoring and
769 Assessment Programme (AMAP), Oslo. 72 pp.
770 Arnold, F., Pirjola, L., Rönkkö, T.,Reichl, U., Schlager, H., Lähde, T., Heikkilä, J., Keskinen, J.,
771 2012. First on-line measurements of sulfuric acid gas in modern heavy duty diesel engine
772 exhaust: Implications for nanoparticle formation, Environ. Sci. Technol. 46, 11227−11234.
773 Arnott, W. P., Hamasha, K., Moosmüller, H., Sheridan, P. J., Ogren, J. A., 2005. Towards aerosol
774 light-absorption measurements with a 7-wavelength aethalometer: evaluation with a
775 photoacoustic instrument and 3-wavelength nephelometer. Aerosol Sci. Technol. 39, 17-29.
776 Asbach, C., Fissan, H., Stahlmecke, B., Kuhlbusch, T., Pui, D., 2009. Conceptual limitations and
777 extensions of lung-deposited nanoparticle surface area monitor (NSAM). J. Nanopart. Res. 11
778 (1), 101-109.
779 Aurela, M., Saarikoski, S., Niemi, J. V., Canonaco, F., Prevot, A., S. H., Frey, A., Carvone, S.,
780 Kousa, A., Hillamo, R., 2015. Chemical and source characterization of submicron particles at

residential and traffic sites in the Helsinki Metropolitan area, Finland. Aerosol and Air Quality Research 15, 1213-1226.

Birmili W, Tomsche L, Sonntag A, Opelt C, Weinhold K, Nordmann S, et al., 2013. Variability of aerosol particles in the urban atmosphere of Dresden (Germany): effects of spatial scale and particle size. Meteorol Z 2013;22:195–211.

Bond, T. C., Doherty, S. J., Fahey, D. W., Forster, P. M., Berntsen, T., DeAngelo, B. J., Flanner, M. G., Ghan, S., Kärcher, B., Koch, D., Kinne, S., Kondeo, Y., Quinn, P. K., Sarofim, M. C., Schultz, M. G., Schulz, M., Venkataraman, C., Zhang, H., Zhang, S., Bellouin, N., Guttikunda, K., Hopke, P. K., Jacobson, M. Z., Kaiser, J. W., Klimont, Z., Lohmann, U., Schwarz, J. P., Shindell, D., Storelvmo, T., Warren, S. G., Zender, C. S., 2013. Bounding the role of black carbon in the climate system: A scientific assessment, J. Geophys. Res.-Atmos. 118, 5380–5552, doi:10.1002/jgrd.50171.

Brown, D., Wilson, M., MacNee, W., Stone, V., Donaldson, K., 2001. Size-dependent proinflammatory effects of ultrafine polystyrene particles: a role for surface area and oxidative stress in the enhanced activity of ultrafines. Toxicol. Appl. Pharmacol. 175, 191-199.

Canagaratna M.R., Jayne J.T., Ghertner D.A., Herndon S., Shi Q., Jimenez J.L., Silva P.J., Williams P., Lanni T., Drewnick F., Demerjian K.L., Kolb C.E. and Worsnop D.R. (2004) Chase studies of particulate emissions from in-use New York City vehicles. Aerosol Sci. Tech., 38, 555–573.

Canagaratna, M.R., Jayne, J.T., Jimenez, J.L., Allan, J.D., Alfarra, M.R., Zhang, Q., Onasch, T.B., Drewnick, F., Coe, H., Middlebrook, A., Delia, A., Williams, L.R., Trimborn, A.M., Northway, M.J., DeCarlo, P.F., Kolb, C.E., Davidovits, P. and Worsnop, D.R. (2007). Chemical and Microphysical Characterization of Ambient Aerosols with the Aerodyne Aerosol Mass Spectrometer. Mass Spectrom. Rev. 26: 185–222.

Canagaratna M.R., Jimenez J.L, Kroll J.H., Chen Q., Kessler S. H., Massoli P, Hildebrandt Ruiz L., Fortner E., Williams L.R., Wilson K.R., Surratt J.D., Donahue N.M., Jayne J.T. and Worsnop D.R. (2015). Elemental ratio measurements of organic compounds using aerosol mass spectrometry: characterization, improved calibration, and implications. Atmos. Chem. Phys. 15: 253–272.

Carbone, S., Aurela, M., Saarnio, K., Saarikoski, S., Timonen, H., Frey, A., Sueper, D., Ulbricht, I., Jimenez, J., Kulmala, M., Worsnop, D., Hillamo, R., 2014. Wintertime Aerosol Chemistry in Sub-Arctic Urban Air. Aerosol Sci. Technol. 48, 313-323.

Crippa, M., et al. (2013), Identification of marine and continental aerosol sources in Paris using high resolution aerosol mass spectrometry, J. Geophys. Res. Atmos., 118, 1950-1963, doi:10.1002/jgrd.50151.

Cubison M.J., Ortega A.M., Hayes P.L., Farmer D.K., Day D., Lechner M.J., Brune W.H., Apel E., Diskin G.S., Fisher J.A., Fuelberg H.E., Hecobian A., Knapp D.J., Mikoviny T., Riemer D., Sachse G.W., Sessions W., Weber R.J., Weinheimer A.J., Wisthaler A. and Jimenez J.L. (2011) Effects of aging on organic aerosol from open biomass burning smoke in aircraft and laboratory studies, Atmos. Chem. Phys. 11, 12049–12064.

DeCarlo, P. F., Kimmel, J. R., Trimborn, A., Northway, M. J., Jayne, J. T., Aiken, A. C., Gonin, M., Fuhrer, K., Horvath, T., Docherty, K. S., Worsnop, D. R., Jimenez, J. L., 2006. Field-deployable, high-resolution, time-of-flight mass spectrometer, Anal. Chem. 78, 8281–8289.

Denier van der Gon, H. A. C., Bergström, R., Fountoukis, C., Johansson, C., Pandis, S. N., Simpson, D., Visschedijk, A. J. H., 2015. Particulate emissions from residential wood combustion in Europe – revised estimates and an evaluation. Atmos. Chem. Phys., 15, 6503–6519, doi:10.5194/acp-15-6503-2015.

EEA Report No 5, 2015. Available at: http://www.eea.europa.eu/publications/air-quality-in-europe-2015.

Enroth, J., Saarikoski, S., Niemi, J., Kousa, A., Ježek, I., Močnik, G., Carbone, S., Kuuluvainen, H., Rönkkö, T., Hillamo, R., Pirjola, L., 2016. Chemical and physical characterization of traffic particles in four different highway environments in the Helsinki metropolitan area. Atmos. Chem. Phys. 16, 5497-5512, doi:10.5194/acp-16-5497-2016.

Favez, O., El Haddad, I., Piot, C., Boréave, A., Abidi, E., Marchand, N., Jaffrezo. J.-L., Besombes, J.-L., Personnaz, M.-B., Sciare, J., Wortham, H., George, C., D'Anna, B., 2010. Inter-comparison of source apportionment models for the estimation of wood burning aerosols during wintertime in an Alpine city (Grenoble, France). Atmos. Chem. Phys. 10, 5295–5314.

Fissan, H., Neumann, S., Trampe, A., Pui, D., Shin, W., 2007. Rationale and principle of an instrument measuring lung deposited nanoparticle surface area. J. Nanopart. Res. 9 (1), 53-59.

Hand, J. L., Malm, W. C., Laskin, A., Day, D., Lee, T., Wang, C., Carrico, C., Carrillo, J., Cowin, J. P., Collet, Jr., J., Iedema, M. J., 2005. Optical, physical and chemical properties of tar balls observed during the Yosemite Aerosol Characterisation Study. J. Geophys. Res. 110, D21210, doi:10.1029/2004JD005728.

Happonen, M., Mylläri, F., Karjalainen, P., Frey, A., Saarikoski, S., Carbone, S., Hillamo, R., Pirjola, L., Häyrinen, A., Kytömäki, J., Niemi, J. V., Keskinen, J., Rönkkö, T., 2013. Size

distribution, chemical composition, and hygroscopicity of fine particles emitted from an oil-fire heating plant. Environ. Sci. Technol. 47, 14468-14475.

Heal, M. R., Kumar, P, Harrison, R. M., 2012. Particles, air quality, policy and health. Chem Soc Rev. 41, 6606–6630.

Heikkilä, J., Rönkkö, T., Lähde, T., Lemmetty, M., Arffman, A., Virtanen, A., Keskinen, J., Pirjola, L., Rothe, D., 2009. Effect of open channel filter on particle emissions of modern diesel engine, J. Air & Waste Manage. Assoc. 59, 1148-1154, DOI:10.3155/1047-3289.59.10.1148.

Hirdman, D., Sodemann, H., Eckhardt, S., Burkhart, J. F., Jefferson, A., Mefford, T., Quinn, K., Sharma, S., Ström, J., Stohl, A., 2010. Source identification of short-lived air pollutants in the Arctic using statistical analysis of measurement data and particle dispersion model output. Atmos. Chem. Phys. 10, 669–693, doi:10.5194/acp-10-10453-2010.

Hoffer, A., Tóth, A., Nyirő-Kósa, I., Pósfai, M., Gelencsér, A., 2016. Light absorption properties of laboratory-generated tar ball particles. Atmos. Chem. Phys. 16, 239-246.

Hovorka, J., Pokorná, P., Hopke, P. K., Křumal, K., Mikuška, P., Píšová, M., 2015. Wood combustion, a dominant source of winter aerosol in residential district in proximity to a large automobile factory in Central Europe. Atmos. Environ. 113, 98-107.

Hussein, T., Hämeri, K., Aalto, P. P., Paatero, P., Kulmala, M., 2005. Modal structure and spatial–temporal variations of urban and suburban aerosols in Helsinki—Finland. Atmos. Environ. 39, 1655-1668.

IPCC, 2013: Climate Change 2013, The Phycical Science Basis, Working Group I, Switzerland, https://www.ipcc.ch/pdf/assessment-report/ar5/wg1/WGIAR5_SPM_brochure_en.pdf.

Jeong, C.-H., Wang, J. M., Evans, G. J. 2016. Source apportionment of urban particulate matter using hourly resolved trace metals, organics, and inorganic aerosol components. Atmos. Chem. Phys. Discuss., doi:10.5194/acp-2016-189.

Karjalainen, P., Ntziachristos, L., Murtonen, T., Wihersaari, H., Simonen, P., Mylläri, F., Nylund, N.-O., Keskinen, J., Rönkkö, T., 2016. Heavy Duty Diesel Exhaust Particles during Engine Motoring Formed by Lube Oil Consumption. Environ. Sci. Technol. 50, 12504-12511, DOI: 10.1021/acs.est.6b03284.

Kaski, N., Aarnio, P., Loukkola, K., Portin, H., 2016. Air quality in the Helsinki metropolitan area in 2015. HSY's publications 6/2016. Helsinki Region Environmental Services Authority.

Kerminen, V.-M., Niemi, J. V., Timonen, H., Aurela, M., Frey, A., Caborone, S., Saarikoski, S., Teinilä, K., Hakkarainen, J., Tamminen, J., Vira, J., Prank, M., Sofiev, M., Hillamo, R., 2011.

879 Characterization of a volcanic ash episode in southern Finland caused by the Grimsvötn
880 eruption in Iceland in May 2011. Atmos. Chem. Phys. 11, 12227–12239.
881 Keskinen, J., Pietarinen, K., and Lehtimäki, M., 1992. Electrical low pressure impactor. J.Aerosol
882 Sci. 23, 353–360.
883 Kittelson, D. B., 1992. Engines and nanoparticles: A review. J. Aerosol Sci. 29, 575−588.
884 Kittelson, D. B., Watts, W. F., Johnson, J. P., Thorne, C., Higham, C., Payne, J., Goodier, S.,
885 Warrens, C., Preston, H., Zink, U., Pickles, D., Goersmann, C., Twigg, M. V., Walker, A. P.,
886 Boddy, R., 2008. Effect of fuel and lube oil sulfur on the performance of a diesel exhaust gas
887 continuously regenerating trap, Environ. Sci. Technol. 42, 9276−9282.
888 Kreckl, P., Larsson, E. H., Ström, J., Johansson, C., 2008. Contribution of residential wood
889 combustion and other sources to hourly winter aerosol in Northern Sweden determined by
890 positive matrix factorization. Atmos. Chem. Phys. 8, 3639–3653.
891 Kumar, P., Fennel, P., Britter, R., 2008. Measurements of particles in the 5–1000 nm range close
892 to road level in an urban street canyon. Sci. Tot. Environ, 390, 437-447.
893 Kupiainen, K., Ritola, R, Stojiljkovic, A., Pirjola, L., Malinen, A., Niemi, J., 2016. Contribution of
894 pavement and traction sanding to road side ambient and suspension PM10 samples. Atmos.
895 Environ. 147, 178−189.
896 Kuuluvainen, H., Rönkkö, T., Järvinen, A., Saari, S., Karjalainen, P., Pirjola, L., Niemi, J. V.,
897 Hillamo, R., Keskinen, J., 2016. Lung deposited surface area size distribution of particulate
898 matter in different urban areas. Atmos. Environ. 136, 105-113.
899 Lanz, V. A., Prévot, A. S. H., Alfarra, M. R., Weimer, S., Mohr, C., DeCarlo, P. R., Gianini, M. F.
900 D., Hueglin, C., Schneider, J., Favez, O., D'Anna, B. D., George, C., Baltensperger, U., 2010.
901 Characterization of aerosol chemical composition with aerosol mass spectrometry in Central
902 Europe: an overview. Atmos. Chem. Phys. 10, 10453–10471, doi:10.5194/acp-10-10453-2010.
903 Lin, Y.-C., Tsai, C.-J., Wu, Y.-C., Zhang, R., Chi, K.-H., Huang, Y.-T., Lin, S.-H., Hsu, S.-C.
904 2015. Characteristics of trace metals in traffic-derived particles in Hsuehshan Tunnel, Taiwan:
905 size distribution, potential source, and fingerprinting metal ratio. Atmospheric Chemistry and
906 Physics 15: 4117-4130. doi:10.5194/acp-15-4117-2015.
907 Liu, C., Chung, C .E., Zhang, F., Yin, Y. 2016. The colors of biomass burning aerosols in the
908 atmosphere. Scientific Reports 6, 28267; doi: 10.1038/srep28267.
909 Marjamäki, M., Ntziachristos, L., Virtanen, A., Ristimäki, J., Keskinen,J., Moisio, M., Palonen,
910 M., and Lappi, M.: Electrical Filter Stage for the ELPI. Society of Automotive Engineers
911 (SAE) Technical Paper 2002–01–0055, 2002.

912 Martinsson, J., Eriksson, A. C., Elbæk Nielsen, I., Berg Malmborg, V., Ahlberg, E., Andersen, C.,
913 Lindgren, R., Nyström, R., Nordin, E. Z., Brune, W. H., Svenningsson, B., Swietlicki, E.,
914 Boman, C., Pagels, J.H., 2015. Impacts of combustion conditions and photochemical
915 processing on the light absorption of biomass combustion aerosol. Environmental Science &
916 Technology 49, 14663-14671.
917 Mohr, C., Richter, R., DeCarlo, P. F., Prévot, A. S. H., Baltensperger, U., 2011. Spatial variation
918 of chemical composition and sources of submicron aerosol in Zurich during wintertime using
919 mobile aerosol mass spectrometer data. Atmos. Chem. Phys. 11, 7465–7482, doi:10.5194/acp-
920 11-7465-2011.
921 Mohr, C., DeCarlo, P.F., Heringa, M.F., Chirico, R., Slowik, J.G., Richter, R., Reche, C.,
922 Alastuey, A., Querol, X., Seco, R., Peñuelas, J., Jiménez, J.L., Crippa, M., Zimmermann, R.,
923 Baltensperger, U., Prévôt, A.S.H., 2012. Identification and Quantification of Organic Aerosol
924 from Cooking and Other Sources in Barcelona Using Aerosol Mass Spectrometer Data.
925 Atmos. Chem. Phys. 12, 1649–1665.
926 Naeher, L. P., Brauer, M., Lipsett, M., Zelikoff, J. T., Simpson, C. D., Koenig, J. Q., and Smith,
927 K. R.: Woodsmoke health effects: A review, Inhal. Toxicol., 19, 67–106,
928 doi:10.1080/08958370600985875, 2007.
929 Ng, N. L., Canagaratna, M. R., Jimenez, J. L., Zhang, Q., Ulbrich, I. M., Worsnop, D. R., 2011.
930 Real-Time Methods for Estimating Organic Component Mass Concentrations from Aerosol
931 Mass Spectrometer Data. Environ. Sci. Technol. 45, 910–916.
932 Niemi, J. V., Tervahattu, H., Virkkula, A., Hillamo, R., Teinilä, K., Koponen, I. K., Kulmala,
933 M.,2005. Continental impact on marine boundary layer coarse particles on Atlantic Ocean
934 between Europe and Antarctica. Atmospheric Research 75, 301-321.
935 Niemi, J. V., Saarikoski, S., Tervahattu, H., Mäkelä, T., Hillamo, R., Vehkamäki, H., Sogacheva,
936 L., Kulmala, M. 2006. Changes in background aerosol composition in Finland during polluted
937 and clean periods studied by TEM/EDX individual particle analysis. Atmospheric Chemistry
938 and Physics 6: 5049-5066.
939 Niemi, J. V., Saarikoski, S., Aurela, M., Tervahattu, H., Hillamo, R., Westphal, D. L., Aarnio, P.,
940 Koskentalo, T., Makkonen, U., Vehkamäki, H., Kulmala, M., 2009. Long-range transport episodes of
941 fine particles in southern Finland during 1999-2007. Atmos. Environ. 43, 1255-1264.
942 Oberdörster, G., Oberdörster, E., Oberdörster, J., 2005. Nanotoxicology: an emerging discipline
943 evolving from studies of ultrafine particles. Environ. Health Perspect. 113, 823-839.

Onasch, T. B., Trimborn, A., Fortner, E. C., Jayne, J. T., Kok, G. L., Williams, L. R., Davidovits, P., Worsnop, D. R., 2012. Soot Particle Aerosol Mass Spectrometer: Development, Validation, and Initial Application, Aerosol Sci. Technol. 46, 804–817.

Paatero P., 1997. Least squares formulation of robust non-negative factor analysis. Chemometr. Intell. Lab. 37, 23-35.

Pirinen, P., Simola, H., Aalto, J., Kaukoranta, J.-P., Karlsson, P., Ruuhela, R., 2012. Climatological statistics of Finland 1981-2010. Reports 2012:1. Finnish Meteorological Institute, Helsinki. 83 pp.

Pirjola, L., Parviainen, H., Hussein, T., Valli, A., Hämeri, K., Aalto, P., Virtanen, A., Keskinen, J., Pakkanen, T., Mäkelä, T., and Hillamo, R., 2004. Atmos. Environ. 38, 3625-3635.

Pirjola, L., Lähde, T., Niemi, J.V., Kousa, A., Rönkkö, T., Karjalainen, P., Keskinen, J., Frey, A., and Hillamo, R.: Spatial and temporal characterization of traffic emission in urban microenvironments with a mobile laboratory. Atmos. Environ. 63, 156-167, 2012.

Pirjola, L., Dittrich, A., Niemi, J. V., Saarikoski, S., Timonen, H., Kuuluvainen, H., Järvinen, A., Kousa, A., Rönkkö, T., Hillamo, R., 2016. Physical and chemical characterization of real-world particle number and mass emissions from city buses in Finland. Environ. Sci. Technol. 50, 294-304.

Pope, C.A., III, and Dockery, D.W., 2006. Health effects of fine particulate air pollution: Lines that connect. J. Air Waste Manage. Assoc.**,** 56, 707-742.

Pósfai, M., Gelencser, A., Simonics, R., Arato, K., Li, J., Hobbs, P. V., Buseck, P. R., 2004. Atmospheric tar balls: Particles from biomass and biofuel burning. Journal of Geophysical Research 109, D06213, doi:10.1029/2003JD004169.

Poulain,L. Iinuma, Y., Müller, K., Birmili, W., Weinhold, W., Brüggemann, E., Gnauk, T., Hausmann, A., Löschau, G., Wiedensohler, A., Herrmann, H., 2011. Diurnal variations of ambient particulate wood burning emissions and their contribution to the concentration of Polycyclic Aromatic Hydrocarbons (PAHs) in Seiffen, Germany, Atmos. Chem. Phys. 11, 12697–12713, doi:10.5194/acp-11-12697-2011.

Quinn, P. K., Bates, T. S., Baum, E., Doubleday, N., Fiore, A. M., Flanner, M., Fridlind, A., Garrett, T. M., Koch, D., Menon, S., Shindell, D., Stohl, A., Warren, S. G., 2008. Short-lived pollutants in the Arctic: their climate impact and possible mitigation strategies. Atmos. Chem. Phys. 8, 1723–1735.

975 Rönkkö, T., Virtanen, A., Kannosto, J., Keskinen, J., Lappi, M., Pirjola, L., 2007. Nucleation
976 mode particles with a non-volatile core in the exhaust of a heavy duty diesel vehicle. Environ.
977 Sci. Technol. 41, 6384-6389 (10.1021/es0705339).
978 Rönkkö, T., Arffman, A., Karjalainen, P., Lähde, T., Heikkilä, J., Pirjola, L., Rothe, D., Keskinen,
979 J., 2011. Diesel exhaust nanoparticle volatility studies by a new thermodenuder with low solid
980 nanoparticle losses, Abstracts in the 15th ETH-Conference on Combustion Generated
981 Nanoparticles, 26–29 June 2011, Zürich, Switzerland.
982 Rönkkö, T., Pirjola, L., Ntziachristos, L., Heikkilä, J., Karjalainen, P., Hillamo, R., Keskinen, J.,
983 2014. Vehicle engines produce exhaust nanoparticles even when not fuelled. Environ. Sci.
984 Technol. 48, 2043−2050, dx.doi.org/10.1021/es405687m.
985 Saari, S., Niemi, J. V., Rönkkö, T., Kuuluvainen, H., Järvinen, A., Pirjola, L., Aurela, M.,
986 Hillamo, R., Keskinen, J., 2015. Seasonal and diurnal variations of fluorescent bioaerosol
987 concentration and size distribution in the urban environment. Aeros. Air Qual. Res. 15, 572-
988 581.
989 Saarikoski, S., Timonen, H., Saarnio, K., Aurela, M., Järvi, L., Keronen, P., Kerminen, V.-M.,
990 Hillamo, R., 2008. Sources of organic carbon in fine particulate matter in northern European
991 urban air. Atmos. Chem. Phys. 8, 6281–6295.
992 Saarnio, K., Niemi, J.V, Saarikoski, S., Aurela, M., Timonen, H., Teinilä, K., Myllynen, M., Frey,
993 A., Lamberg, H., Jokiniemi, J., Hillamo, R. 2012. Using monosaccharide anhydrides to
994 estimate the impact of wood combustion on fine particles in the Helsinki Metropolitan Area,
995 Bor. Env. Res. 17, 163-183.
996 Sandradewi, J., Prévót, A. S. H., Weingartner, E., Schmidhauser, R., Gysel, M., Baltensperger, U.,
997 2008. A study of wood burning and traffic aerosols in an Alpine valley using a multi-
998 wavelength Aethalometer, Atmos. Environ., 42, 101−112.
999 Savolahti, M., Karvosenoja, N., Tissari, J., Kupiainen, K., Sippula, O., Jokiniemi, J., 2016. Black
1000 carbon and fine particle emissions in Finnish residential wood combustion: Emission
1001 projections, reduction measures and the impact of combustion practices, Atmos. Environ. 140,
1002 495–505.
1003 Schneider, J., Hock, N., Weimer, S., Borrmann, S., Kirchner, U., Vogt, R., Scheer, V., 2005.
1004 Nucleation particles in diesel exhaust: Composition inferred from in situ mass spectrometer
1005 analysis. Environ. Sci. Technol. 39, 6153−6161.
1006 Sillanpää, M., Saarikoski, S., Hillamo, R., Pennanen, A., Makkonen, U., Spolnik, Z., Van
1007 Grieken, T., Koskentalo, T., Salonen, R. O., 2005. Chemical composition, mass size

distribution and source analysis of long-range transported wildfire smokes in Helsinki, Science of the Total Environment 350, 119-135.

Stein, A.F., Draxler, R.R, Rolph, G.D., Stunder, B.J.B., Cohen, M.D., and Ngan, F., 2015. NOAA's HYSPLIT atmospheric transport and dispersion modeling system. Bull. Amer. Meteor. Soc. 96, 2059-2077, http://dx.doi.org/10.1175/BAMS-D-14-00110.1.

Su, D. S., Serafino, A., Müller, J.-O., Jentoft, R. E., Schlögl, R., Fiorito, S., 2008. Cytotoxicity and Inflammatory Potential of Soot Particles of Low-Emission Diesel Engines. Environ. Sci. Technol. 42, 1761−1765.

Timonen, H., Carbone, S., Aurela, M., Saarnio, S., Saarikoski, S., Nga, L. N., et al. (2013). Characteristics, Sources and Water-Solubility of Ambient Submicron Aerosol in Springtime in Helsinki, Finland. *J. Aerosol Sci.* 56:61–77.

Tobias, H., Beving, D., Ziemann, P., Sakurai, H., Zuk, M., McMurry, P., Zarling, D., Watylonis, R., Kittelson, D., 2001. Chemical analysis of diesel engine nanoparticles using a nano-DMA/thermal desorption particle beam mass spectrometer. Environ. Sci. Technol. 35, 2233−2243.

Torvela, T., Tissari, J., Sippula, O., Kaivosoja, T., Leskinen, J., Virén, A., Lähde, A., Jokiniemi, J. 2014. Effect of wood combustion conditions on the morphology of freshly emitted fine particles. Atmospheric Environment 87, 65-76.

Ulbrich, I. M., Canagaratna, M. R., Zhang, Q., Worsnop, D. R., Jimenez, J. L. (2009). Interpretation of organics components from Positive Matrix Factorization of aerosol mass spectrometric data. Atmos. Chem. Phys. 9: 2891–2918.

Uski, O., Jalava, P., Happo, M., Torvela, T., Leskinen, J., Mäki-Paakkanen, J., Tissari, J., Sippula, O., Lamberg, H., Jokiniemi, J., Hirvonen M.-R. 2015. Effect of fuel zinc content on toxicological responses of particulate matter from pellet combustion in vitro. Science of the Total Environment 511: 331-340.

Virkkula, A., Mäkelä, T., Hillamo, R., Yli-Tuomi, T., Hirsikko, A., Hämeri, K., Koponen, I., 2007. A simple procedure for correcting loading effects of aethalometer data. Journal of the Air &Waste Management Association 57, 1214-1222.

Weimer, S., Mohr, C., Richter, R., Keller, J., Mohr, M., Prévót, A.S. H., Baltensperger, U., 2009. Mobile measurements of aerosol number and volume size distribution in an Alpine valley: Influence of traffic versus wood burning. Atmos. Environ. 43, 624-630.

Yli-Ojanperä, J., Kannosto, J., Marjamäki, M., and Keskinen, J., 2010. Improving the nanoparticle resolution of the ELPI. Aerosol and Air Quality Research 10, 360-366.

1041 Zhang, Q., Worsnop, D. R., Canagaratna, M. R., Jimenez1, J. L., 2005. Hydrocarbon-like and
1042 oxygenated organic aerosols in Pittsburgh: insights into sources and processes of organic
1043 aerosols. Atmos. Chem. Phys.5, 3289–3311.
1044 Zhang Q., Jimenez J.L., Canagaratna M.R., Ulbrich I.M., Ng N.L., Worsnop D.R. Sun Y., 2011.
1045 Understanding atmospheric organic aerosols via factor analysis of aerosol mass spectrometry:
1046 a review. Anal. Bioanal. Chem. 401, 3045-3067.
1047
1048